

Manuscript: "Spectral Sizing of a Coarse Spectral Resolution Satellite Sensor for XCO₂"
by JS Wilzewski et al.

Reply to interactive comment by anonymous reviewer #1

We thank the reviewer for the helpful comments to our manuscript. Below we repeat the reviewer's questions in **bold** font and subsequently provide our responses.

1. It is unclear to me how column mean dry air mole fractions of CO₂ are obtained in a retrieval without NIR band, i.e. in a retrieval where no O₂ column is estimated. Where is the information on O₂ taken from? From surface pressures from a weather prediction model? How does that add to the overall uncertainty? Isn't the retrieval very sensitive to topographic variations and thus to the pointing accuracy of the instrument in this case?

Column averaged dry air mole fractions of CO₂, XCO₂, are calculated by deviding the retrieved CO₂ concentrations by the airmass below the satellite. In our work, the airmass is determined from a global digital elevation model (NASA's Shuttle Radar Tomography Mission – SRTM) together with surface pressure reanalyses from ECMWF (ERA Interim). This is the standard way how our native RemoTeC algorithm works for trace gas retrievals from the GOSAT, OCO-2 and TROPOMI satellite instruments.

The point raised in your comment about pointing accuracy is very important. Naturally, if our proposed instrument was pointed towards a target site on a terrain with a great slope, pointing errors would be translated into elevation errors/XCO₂ errors (20 m of elevation error would result in roughly 1 ppm of XCO₂ error). Thus, errors in the calculation of the airmass are part of the overall uncertainty found in our analysis. But, these error contributions are equal for the native and reduced-resolution retrievals because the calculation of airmass is the same. In fact, not shown in the paper, we tried to refine our analysis by looking at localized signals above the urban area of Los Angeles. There, we found that uncertainties in GOSAT's pointing can induce significant errors related to the airmass calculation.

To clarify how airmass is obtained, we added the following on page 7, line 23 – 28: "For both, native GOSAT and degraded SWIR configurations, airmass information is derived from ECMWF surface pressure reanalyses (ERA-Interim) and topographic data from the Shuttle Radar Tomography Mission (SRTM). For each sounding, we use ECMWF and SRTM data to cal-

culate the ground-pixel average surface pressure and the corresponding dry airmass.. This is the standard operation procedure for RemoTeC trace gas retrievals from the GOSAT, OCO-2 and TROPOMI satellite instruments. Errors in the calculation of the airmass can be caused by erroneous satellite pointing; these errors are part of the overall errors reported for the TCCON validation sites (section 3).”

2. A problem not really addressed in the study is the fact that coarser spectral resolution instruments tend to have larger uncertainties in the spectral calibration. The retrieval can account for spectral shifts, but this is more difficult in case of coarsely resolved spectra. What were the assumptions regarding spectral calibration uncertainties and how would that affect the conclusions?

There were no assumptions regarding spectral calibration uncertainties in this study. Spectral shifts are free parameters in our retrieval for both, the native and the reduced resolution setups. We start with the standard spectral calibration provided in the GOSAT L1B data files. Then, the retrievals shift the simulated observations to minimize the least-squares difference to the observations. Any errors caused by interferences of adjusting the spectral shifts and fitting XCO₂ are contributors to the errors that we discuss in the paper. However, we have no indication (e.g. particularly large uncertainties of the spectral shift parameters) that spectral shifting is a large error contribution.

3. Only quality-screened cloud-free GOSAT spectra were used in the analysis. How much does that screening depend on the information in the NIR and SWIR channels? Or in other words, how much more difficult would quality/cloud screening be for an instrument with a single SWIR channel? This seems important to me, since only a small proportion of pixels usually survive the strict quality flagging required for satellite CO₂ retrievals.

The question of quality screening has not been addressed in this study. Unfortunately, we cannot afford the computational costs to reprocess the entire GOSAT dataset (including all the cloudy data) of the years 2009 to 2016 that we used in the study. Thus, we cannot give a quantitative reply to this remark, but we argue that while cloud detection would certainly be more challenging with a coarse resolution 1-Band configuration, the SWIR-2 spectral range offers the possibility to construct a decent cloud filter. To this end, one could make use of the two CO₂ bands in this window, which have

the advantage of having very different optical depths. XCO₂ retrievals from either band should then be consistent in cloud-free scenes and different in complicated scenes. Yet, to assess this screening procedure, a follow up study is necessary.

We now mention in the paper that we did not carry out a cloud filtering exercise on page 5, line 8: “Due to computational costs, we restrict our analysis to cloud-free, quality screened soundings over land as identified by the native GOSAT retrievals of the RemoTeC algorithm...”.

Also, we added a discussion of the SWIR cloud filter option in the discussion (page 18, line 4 – 8): “Additionally, the SWIR-2 seems better suited for the construction of a cloud filter, because its CO₂ bands have very different optical depths. Similar to the cloud filter currently in use for GOSAT measurements, one could retrieve XCO₂ from the two SWIR-2 bands individually and filter for discrepancies. This scheme should be tested in the future.”

Since the main application of the sensor will be point-source detection and quantification, a future study should focus on local rather than global scales as done here. The recent study of Cusworth et al. (2019; <https://doi.org/10.5194/amt-2019-202>), for example, shows that local plume detection can be significantly affected by retrieval errors which are correlated with surface reflectance. The spectral resolution of the instrument proposed here may be high enough to mitigate such problems, but this aspect should receive more attention in a future study.

Thank you for pointing out the study by Cusworth et al., which we now cite in the discussion (page 17, line 30): “Surface reflectance has been shown to be a central driver in methane retrieval precision by Cusworth et al. (2019)”. We also agree that local scale phenomena related to surface reflectance and plume detection need to be investigated further in coming studies.

Manuscript: "Spectral Sizing of a Coarse Spectral Resolution Satellite Sensor for XCO₂"
by JS Wilzewski et al.

Reply to interactive comment by anonymous reviewer #2

We thank the reviewer for the helpful comments to our manuscript. Below we repeat the reviewer's questions in **bold** font and subsequently provide our responses.

General Comments

The authors traded-off the spectral resolution but performance with and without O₂A is not clear. Did they consider an O₂A spectrometer with moderate spectral resolution?

We realize that knowledge of particle scattering in the atmosphere would be improved by observing the oxygen A-Band. Any information, even at coarse spectral resolution, on O₂ absorption in the NIR would be useful to characterize aerosol properties. However, we have not considered an additional spectrometer as this would significantly increase cost and mass of the proposed instrument that we envision to be employed in fleets of relatively inexpensive and small satellites. In terms of possibly losing performance due to uncertainties in the airmass, because of our one band set-up, we would like to emphasize that RemoTeC does not rely on the O₂ A-band to calculate airmass. Instead, information from prior topography and meteorology (such as surface pressure values from the ERA Interim product by ECMWF) is used to determine the air mass below the satellite.

A short discussion of how RemoTeC calculates airmass was added on page 7, line 23 – 27: "For both, native GOSAT and degraded SWIR configurations, airmass information is derived from ECMWF surface pressure reanalyses (ERA-Interim) and topographic data from the Shuttle Radar Tomography Mission (SRTM). For each sounding, we use ECMWF and SRTM data to calculate the ground-pixel average surface pressure and the corresponding dry airmass.. This is the standard operation procedure for RemoTeC trace gas retrievals from the GOSAT, OCO-2 and TROPOMI satellite instruments."

GOSAT has measured several data over cities such as Tokyo and LA using its target observation function. The authors can pick up and discuss aerosol effect over cities.

We investigated the possibility to focus on localized signals by looking at

target observations of the Los Angeles basin. However, the data were still too sparse to evaluate the effect of aerosols in a significant matter.

They also concluded that dust is the largest error source by specifying latitudinal ranges. GOSAT has observed desert area such as Sahara and Arabian Desert with its medium gain. The authors can analyze directly by picking up medium gain data

Our analysis shows that errors correlate with the desert latitudes. This is apparent from our analysis, which is based on a mix of high and medium gain spectra (medium gain measurements account for ca. 12 % of the dataset). We do not see what additional information an analysis of medium gain data alone would provide.

Specific Comments

(1) Page 1, Abstract The spectral resolution coarser than native GOSAT and the single-band of CO2 without O2A band are both key parts of this study. However, the latter is not clearly mentioned in the abstract.

We have emphasized that we carry out single-band retrievals in the abstract (page 1, line 11): "...and we evaluate single-band retrievals...".

(2) page 6, Line 18, "non-scattering retrieval", Page 8, Line 9, "the non-scattering SWIR-1 retrieval" Brief description is needed.

Non-scattering retrievals refer to retrievals where scattering by particles is neglected.

We added an explanation (page 6, line 8 – 9): "This approach, which is essentially a transmittance calculation along the geometric lightpath, is hereafter referred to as non-scattering retrieval."

(3) Page 6, Line 20, "More than 75 % of all retrievals converge at any given FWHM that we consider in this study." It is difficult to understand

This statement refers to the fact that the retrieval algorithm converges towards a solution after a reasonable number of iterations for the majority of retrievals we perform. As the degree of freedom for signal for the aerosol parameter retrieval varies with resolving power, the retrieval becomes more or less tightly regularized so that it may not find the global minimum of

the cost function. We added to a sentence in the paper to make this clearer (page 7, line 9 – 10): “Although variations in DFS may lead to changes in the ability of the retrieval algorithm to converge towards the minimum of the cost function, ...”.

(4) Page 7, Line 19, ”1.856%” It is not clear. Is it 1.8% of XCO₂? 7.4 ppm?

To make the spectroscopic cross sections of CO₂ near 2 μm consistent, we apply a scaling factor to the strong CO₂ band. This factor was determined from calculating XCO₂ from the two bands separately. The referee is right that it was not clear which way our scaling of the XCO₂ cross sections at 2.01 μm goes. We added the information in the text (page 8, line 1): “i.e. the cross sections of the 2.01 μm band need to be scaled by 0.981”.

(5) Page 10, Figure 4 Use of three individual figures will become clearer.

We have updated the figure accordingly.

(6) Page 16, Line 30 ”an additional aerosol sensor may help” The largest error source seems to be vertical profile of particles. Conventional aerosol imager provides horizontal distribution only. Which kind of sensor do authors consider?

Ideally, we want an aerosol instrument that provides multi-angle, radiance and polarization information over a wide spectral range (from the UV to the NIR) while the instrument is sufficiently compact to fit on a small satellite. Hasekamp et al. (2019) describe such an instrument to be deployed on the NASA PACE mission (we included a reference to this work in the manuscript on page 17, line 17).

Technical Corrections (1) Page 6, Line 11 XH₂O Definition of ’XH₂O’ should be described

A short description was added in the text (page 5, line 27 – 28): “throughout this work *Xmolecule* refers to the column-averaged dry air mole fraction of a molecule”

(2) Page 12, Figure 12 At present, it is monochromatic. It should be a color figure such as figures 6 and 11. Grey line is difficult to

see.

This Figure was updated with the same color map as Figures 6 and 11.

References

Hasekamp, O. P., Fu, G., Rusli, S. P., Wu, L., Di Noia, A., aan de Brugh, J., Landgraf J., Smit, J. M., Rietjens, J., van Amerongen, A.: Aerosol measurements by SPEXone on the NASA PACE mission: expected retrieval capabilities, *Journal of Quantitative Spectroscopy and Radiative Transfer*, 227, 170 – 184, <https://doi.org/10.1016/j.jqsrt.2019.02.006>

Manuscript: "Spectral Sizing of a Coarse Spectral Resolution Satellite Sensor for XCO₂"
by JS Wilzewski et al.

Reply to interactive comment by anonymous reviewer #3

We thank the reviewer for the helpful comments to our manuscript. Below we repeat the reviewer's questions in **bold** font and subsequently provide our responses.

General Comments

Because these spectrometers will be for local-scale (power plant, urban scale) domains, the global-scale performance of individual GOSAT 10x10 km² really is only a starting point. It would be important to model the potential behavior of such a satellite using an OSSE (Observing System Simulation Experiment) over high-resolution, simulated local-scale domains. The authors should add a (potentially short) discussion of this limitation to the paper.

We agree that most of the analyses performed in this work are just a starting point towards evaluating a possible future CO₂ sensor. It will certainly be crucial to carry out detailed simulations of this proposed spectrometer with a thorough discussion of the actual instrument design and noise performance for representative local-scale domains. In the present manuscript we focus on investigating whether a coarse resolution, single band observation configuration could generally deliver sufficient information such that a meaningful retrieval of XCO₂ can be made. Details of the satellite sensor shall be studied in a forthcoming study, currently under preparation in our group.

We added "A forthcoming study addressing these aspects of the proposed sensor is currently under preparation." in the manuscript on page 18, line 8 – 9.

I have a methodological question as follows. In terms of taking real GOSAT data, and simply convolving it with a wider ILS, it seems like the SNR of the resulting measurement (with 256 channels per band) will be higher than one may actually be able to build in a realistic instrument. For instance, I performed a simulation of simple white noise for 1300 GOSAT channels spaced every 0.2 cm⁻¹ (the approximate channel spacing for GOSAT) between 4740 and 5000 cm⁻¹, and had a starting SNR of 700. In the simulation, when I convolved the spectrum (with realistic noise added) with a Gaussian ILS with FWHM=1.3 nm, the resulting SNR was ~3400. This was due to the averaging effect of the

hi-resolution GOSAT data.

The authors do state (section 2) “Since we want to isolate the effects of spectral resolution and spectral band selection, we do not add extra noise to the convolved spectra.” However, they are worried here about the effect of smaller ground pixels. BUT, it seems they are not taking into account this averaging effect ‘beating down’ the native GOSAT noise to unrealistically high SNR values. Here, the final SNR value of 3400 is NOT equal to the GOSAT value of 700, so I think they are not purely “isolating the effect of spectral resolution” since the SNR values are wildly different. Did the authors examine the resulting SNR of their low-resolution GOSAT measurements, and are they in line with what they would expect from their hypothetical instrument? I realize they somewhat avoid this question by not having a real instrument noise model proposed, but as written, the results may be misleading because they may assume unrealistically high SNR values for any possible instrument. The authors should discuss this point and make it clear. Also, this could be rectified by proposing a realistic instrument noise model, and then ADDING noise to the GOSAT spectrum after convolution with th Gaussian ILS, in order to obtain an SNR in line with a more realistic value.

It is evident that the effect of convolving the native GOSAT spectra with a wider ILS (sampled by 3 detector pixels) results in higher SNR per pixel for the setup with reduced spectral resolution then for the native configuration. And, indeed, we do not compensate for the “beating down” of the noise by adding extra noise (as mentioned by the manuscript).

Adding noise to the spectra would introduce an additional artificial element (besides the coarse ILS) to our analysis. We want to stick as close as possible to real measurements and, as stated by the manuscript, we want to isolate the one effect (i.e. coarse ILS).

Errors in native GOSAT retrievals are not dominated by noise. In fact, an SNR of 700 (at the radiance continuum?) as assumed by the reviewer is by far better than the observed spectral fitting residuals which are for the most part dominated by systematic patterns (unresolved scattering effects, spectroscopic errors, unaccounted instrument characteristics). Likewise, the noise errors on retrieved XCO₂ are typically a factor 2-4 smaller than the standard deviations found when comparing to validation data (see also our figure 12). Thus, for a GOSAT-like setup, noise is a minor contributor to the errors. The noise for convolved and unconvolved spectra might be “wildly” different, but, for both, it is small compared to other sources of error. Accepting that the noise is small makes it straightforward

to evaluate these other sources of error e.g. through the parameter correlations shown in the paper, which we chose to be the focus of the present paper.

Adding noise to the spectra to mimic a new sensor with fine ground resolution would result in a different paper. We would need to discuss the instrument optical and electronic setup and describe the noise model. Such a paper is in preparation including a noise evaluation with simulated data. The present paper aims at discussing whether it is reasonable at all to try out a coarse-spectral-resolution configuration.

Essentially, our results are representative under circumstances where the noise can be assumed small compared to other sources of error. The next paper will address how to build the instrument, for what scenes noise is indeed negligible, and what to expect if noise becomes large for dark surfaces. To make these aspects clear, we add the following paragraph to the manuscript:

“Our approach essentially relates to conditions under which the detector noise is negligible as typical for GOSAT. Under such conditions, other sources of error can be addressed e.g. through evaluating geophysical parameter correlations (section 3 and 4). A forthcoming study will discuss noise performance and retrieval simulations for a hypothetical instrument design.” (page 5, line 20 – 23).

Another concern is the impact of not using the O2A band. The authors should discuss the feasibility of seeing power plant plumes in the face of realistic pointing errors, and if the pointing will be sufficiently good such that surface pressure estimates from meteorological reanalysis, hypsometrically adjusted to account for the local topography, will be a relatively small error or not.

As the proposed sensor will have imaging ability, the spectrometer shows promise to have a good pointing knowledge. Any errors in pointing may be ‘recalibrated’ when scenes with prominent surface reflectance features, such as shorelines, etc., are observed. We expect that even if pointing accuracy is low, one would be able to obtain a good correction in order to correctly calculate airmass for the XCO₂ retrieval.

We added “Errors in the calculation of the airmass can be caused by erroneous satellite pointing; these errors are part of the overall errors reported for the TC-CON validation sites (section 3).” (page 7, line 26 – 27).

A critical concern is the ability to properly filter the data. For many XCO₂ retrievals, cloud and aerosol filtering is a critical component of any retrieval system, yet this is completely left out of this analysis as the authors start with data pre-filtered using the native GOSAT 3-

band retrievals. It is therefore not clear how robust the conclusions would be if the sensor had to solely rely on filtering from a single, low-resolution SWIR band. While this study is a good start, results from a proper simulation-retrieval experiment including the effects of clouds & aerosols and the role of pre-filtering is of critical importance to realistically judge if such a simple sensor could truly determine power plant emissions.

We would have liked to analyze the impact on cloud-screening, however, due to computational costs, we could not. It should be pointed out that the SWIR-2 configuration, which is favored for the future instrument, has two CO₂ absorption bands with very different optical depths, which opens up an avenue to set-up a cloud filter using the SWIR-2 window alone. By retrieving XCO₂ from both CO₂ bands, one could filter for large discrepancies caused by the presence of clouds. This is a variant of the cloud filter currently used for the native GOSAT soundings. The actual implementation and verification of this approach must be postponed to a future study.

We now mention in the paper that we did not carry out a cloud filtering exercise on page 5, line 8: “Due to computational costs, we restrict our analysis to cloud-free, quality screened soundings over land as identified by the native GOSAT retrievals of the RemoTeC algorithm...”.

Also, we added a discussion of the SWIR cloud filter option in the discussion (page 18, line 4 – 7): “Additionally, the SWIR-2 seems better suited for the construction of a cloud filter, because its CO₂ bands have very different optical depths. Similar to the cloud filter currently in use for GOSAT measurements, one could retrieve XCO₂ from the two SWIR-2 bands individually and filter for discrepancies. This scheme should be tested in the future.”

Specific Comments

P5L20: You assume 256 spectral channels in a single band. This seems like a high oversampling rate (~ 3 for both SWIR-1 and SWIR-2), considering that there are roughly 86 fully independent spectral samples in each band, given your proposed resolving powers. This rate appears to have been carefully chosen. Please speak to any knowledge you have on the importance of the spectral oversampling, as it may be an important consideration (for SNR or retrieval accuracy/precision). I just noticed this is also discussed on page 9, but the factor of 3 oversampling is again assumed there, and not questioned or discussed as any kind of instrument parameter to be optimized (in the way that spectral resolution is, in this study).

We have assumed a spectral sampling ratio of three throughout this work. A sampling ratio of 2 would be the lower limit according to Nyquist’s theorem. Generally, the higher the sampling ratio, the better. Detectors with a very high number of pixels (e.g 2000 pixels) could enable a significantly higher sampling ratio. Yet, previous space-based CO₂ missions have been successful by spectrally over-sampling the FWHM by a factor 2-3 (e.g. GOSAT, OCO-2, OCO-3, TanSat). Thus our choice of sampling ratio is based on what is currently in use for similar sensors.

P6L17. The improvement of your 3-aerosol-parameter retrieval vs. a non-scattering retrieval is curious, consider the extremely low DFS for aerosol you cite (0.38). It therefore seems possible that your results may be sensitive to the prior assumption on aerosols. How are the aerosol priors for the 3 parameters chosen, and did you test your sensitivity to the aerosol prior, given the low DFS?

Given that the retrievals estimate 3 aerosol parameters with little DFS, the retrievals, by definition of DFS, depend on the a priori. We have conducted a sensitivity study how various aerosol priors map into XCO₂ errors. As prior aerosol we had selected reasonable numbers for scattering optical depth ($\tau=0.1$), scattering layer height ($z_{par}=3000$ m) and size parameter ($\alpha_{par}=3.5$) throughout the study. These values are routinely used as prior for GOSAT retrievals with RemoTeC. Table 1 shows the changes in scatter around TCCON as well as the changes in correlation coefficients for SWIR-2 retrievals at 1.29 nm resolution with changed aerosol priors. As we only have ~ 0.4 degrees of freedom to be distributed to the fit of three aerosol parameters, it is clear that the aerosol prior can have an impact on retrieval performance.

We find that our results are moderately sensitive to small changes in τ or z_{par} , while larger variations in the prior have a big impact on XCO₂ retrieval performance. For instance, changing τ by a factor 2 or $\frac{1}{2}$ leads to relatively small deviations from our benchmark SWIR-2 retrieval regarding scatter around TCCON and geophysical correlations on a global scale. We observe $\sigma_{TCCON} = 3.19$ ppm for $\tau=0.05$ and $\sigma_{TCCON} = 3.50$ ppm for $\tau=0.2$. Correlation coefficients to albedo and other geophysical parameters (as in Fig. 11 of the manuscript) are collected in Table 1. Changes in retrieval performance also occur for small changes in the initial scattering layer height. For prior layer heights of 1000 m and 5000 m, the standard deviation of SWIR-2 retrievals around colocated TCCON data amounts to 3.32 ppm and 3.71 ppm, respectively. This indicates a stronger dependence on scattering layer height priors than on optical depth priors. A significant change in retrieval performance occurs for a prior aerosol scenario, where rather large scat-

tering particles are placed at the top of the troposphere ($\tau=0.07$ $z_{par}=11600$ m $\alpha_{par}=3.67$). In this case, $\sigma_{TCCON}=4.14$ ppm is higher than for all other aerosol prior options we studied here.

As a result, extreme prior aerosol values have to be avoided for our retrievals. This sensitivity study shows that the retrieval performance of the proposed sensor may be enhanced by a few tenths of a ppm by using a good aerosol prior. An additional aerosol sensor would help to inform and optimize the retrievals.

We added “An investigation of the impact of the aerosol priors on retrieval performance showed that SWIR-2 XCO₂ is only moderately sensitive to the aerosol priors. For instance, varying aerosol prior optical depth by a factor of two or one half resulted in small changes in standard deviations around TCCON (+0.22 ppm and -0.08 ppm, respectively). Changing scattering layer height priors to $z_{par}=1000$ m or $z_{par}=5000$ m increased scatter around TCCON by +0.04 ppm and +0.43 ppm, respectively. Similarly, scatter around TCCON changes by +0.22 ppm and -0.05 ppm if α_{par} is set to 3.0 and 5.0, respectively.” in the manuscript (page 10, line 20 – page 11, line 2).

Aerosol prior	σ_{TCCON} / ppm	R(albedo)	R(SOT)	R(N_{par})	R(z_{par})	R(α_{par})
$\tau=0.1$ $z_{par}=3000$ m $\alpha_{par}=3.5$	3.28	-0.18	0.26	-0.5	0.21	0.01
$\tau=0.07$ $z_{par}=11600$ m $\alpha_{par}=3.67$	4.14	-0.48	0.17	-0.5	0.17	0.09
$\tau=0.05$ $z_{par}=3000$ m $\alpha_{par}=3.5$	3.19	0.04	0.31	-0.45	0.21	-0.07
$\tau=0.2$ $z_{par}=3000$ m $\alpha_{par}=3.5$	3.50	-0.30	0.21	-0.50	0.19	0.07
$\tau=0.1$ $z_{par}=1000$ m $\alpha_{par}=3.5$	3.32	0.20	0.31	-0.4	0.19	-0.11
$\tau=0.1$ $z_{par}=5000$ m $\alpha_{par}=3.5$	3.71	-0.36	0.21	-0.47	0.20	0.06
$\tau=0.1$ $z_{par}=3000$ m $\alpha_{par}=3.0$	3.42	-0.24	0.23	-0.49	0.20	0.07
$\tau=0.1$ $z_{par}=3000$ m $\alpha_{par}=5.0$	3.23	-0.05	0.3	-0.5	0.2	-0.09

Table 1: Comparison of the effect of different aerosol priors on standard deviation of retrieval results around TCCON (σ_{TCCON}) and on the correlation coefficients (“R(X)”) with respect to geophysical parameters (albedo at 2.1 nm, SOT, particle amount, scattering layer height and size parameter) as in Fig. 11 of the manuscript. The highlighted row shows the parameters for the prior with which we have carried out the calculations for the manuscript. The respective aerosol prior is shown in the first column.

Also, is this only for SWIR-2? I would be curious if you attempted scattering retrievals for SWIR-1, to prove that they are no better than non-scattering is right. If my hypothesis is correct, they may be better for the same reason as for SWIR-2? the the information is more from the prior, and not the measurement itself.

We did attempt to include scattering in the SWIR-1 retrievals as mentioned on page 7, line 1 – 2, but even at native GOSAT spectral resolution, a SWIR-1 single band retrieval accounting for scattering typically has an average of 0.24 degrees of freedom for three aerosol parameters. At coarse spectral resolution we encountered low information content and worse retrieval performance with respect to scatter around TCCON. Thus, neglecting aerosol particles in the retrievals seemed the better choice. We added “the SWIR-1 band suffers from low information content and results in worse XCO₂ retrieval performance than under the non-scattering assumption” on page 7, line 2 – 3 in the manuscript.

P7L19: The 1.86% scaling factor is interesting. Which way does it go? e.g., do you require a +1.86% scaling of the gas absorption coefficients at 2.01 to match 2.06? Please state this explicitly, as spectroscopists might be interested.

This was indeed unclear. We have added “(i.e. cross sections of the 2.01 μm band need be scaled by 0.981)” in the manuscript (page 7, line 35) to explain this scaling.

P9: I think it is also important to examine the change in standard deviation (scatter) of GOSAT-TCCON at individual sites, to see if that increases more for some sites over others. The global numbers (3.0 and 3.28 ppm vs. 2.43), but it would be interesting to see what these are for individual sites. This information would be usefully presented in a table. In fact, I think a table is important, where the basic information per site is presented (N, mean bias, Stddev). Currently, you try to graphically represent only the per-site bias (in Figure 5).

This information is indeed useful and we have decided to expand Fig. 5 to also show scatter around TCCON at individual sites (we also changed the caption accordingly). Furthermore, the figure was updated to contain information about the number of colocated soundings at each station. In addition, we added Table 2 in the form of a supplementary material.

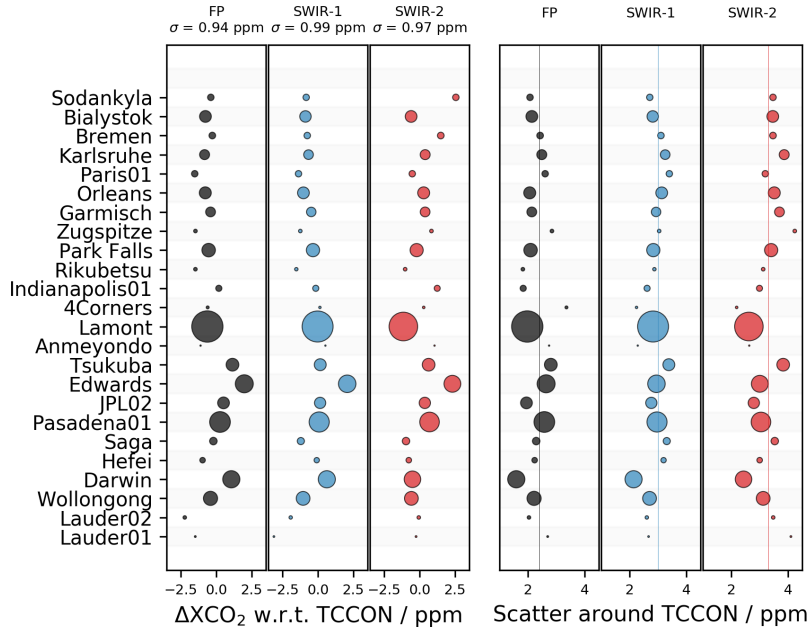


Figure 1: Comparison of retrieval performances at individual TCCON stations sorted north to south. Marker size indicates amount of colocated soundings at each station. Left: Station-by-station mean differences between TCCON and the native (black), SWIR-1 (red), and SWIR-2 (blue) retrievals from GOSAT. The standard deviation of mean differences among the stations, σ , amounts to 0.94 ppm (native), 0.99 ppm (SWIR-1) and 0.97 ppm (SWIR-2). Right: Scatter around TCCON per station for the native, SWIR-1, and SWIR-2 retrievals. Vertical lines mark the average standard deviations (native: 2.43 ppm, SWIR-1: 3.00 ppm, SWIR-2: 3.28 ppm).

We added “Figure 5 also shows XCO₂ retrieval standard deviations per TCCON station. The corresponding data for retrieval performance at individual sites can be found in the supplementary materials.” on page 10, line 1 – 3.

TCCON site	N			Bias / ppm			σ / ppm		
	FP	SWIR-1	SWIR-2	FP	SWIR-1	SWIR-2	FP	SWIR-1	SWIR-2
Sodankyla	217	211	217	-0.38	-0.83	2.55	2.08	2.71	3.47
Bialystok	714	673	708	-0.76	-0.88	-0.6	2.14	2.82	3.46
Bremen	229	218	229	-0.28	-0.75	1.49	2.43	3.11	3.47
Karlsruhe	512	478	512	-0.82	-0.66	0.39	2.49	3.26	3.86
Paris01	215	211	214	-1.52	-1.37	-0.52	2.61	3.4	3.2
Orleans	740	712	736	-0.77	-1.02	0.28	2.06	3.13	3.52
Garmisch	493	462	493	-0.4	-0.47	0.39	2.14	2.93	3.7
Zugspitze	69	66	69	-1.47	-1.24	0.83	2.85	3.04	4.24
Park Falls	940	905	896	-0.53	-0.35	-0.21	2.09	2.84	3.41
Rikubetsu	68	60	68	-1.47	-1.52	-1.02	1.82	2.87	3.12
Indianapolis01	195	193	188	0.18	-0.15	1.24	1.84	2.62	2.99
4Corners	45	30	34	-0.6	0.14	0.29	3.36	2.24	2.19
Lamont	5047	4939	4208	-0.62	-0.02	-1.15	1.98	2.83	2.62
Anmeyondo	9	9	9	-1.1	0.53	1.05	2.75	2.29	2.63
Tsukuba	837	731	830	1.15	0.16	0.63	2.81	3.38	3.83
Edwards	1666	1575	1462	1.98	2.07	2.31	2.64	2.95	3.0
JPL02	713	652	659	0.52	0.15	0.36	1.95	2.77	2.79
Pasadena01	2209	2084	1979	0.27	0.09	0.7	2.58	2.97	3.05
Saga	293	264	287	-0.2	-1.21	-0.96	2.29	3.31	3.53
Hefei	159	148	159	-0.96	-0.09	-0.77	2.24	3.2	3.0
Darwin	1521	1510	1404	1.07	0.63	-0.51	1.59	2.14	2.43
Wollongong	1029	975	974	-0.4	-1.05	-0.58	2.22	2.7	3.12
Lauder02	65	61	65	-2.22	-1.92	-0.06	2.04	2.61	3.48
Lauder01	17	15	17	-1.48	-3.11	-0.25	2.7	2.67	4.1

Table 2: Comparison of full-physics (FP), SWIR-1 and SWIR-2 retrievals for soundings colocated with individual TCCON stations. Stations are sorted north to south in the first column. Number of soundings (second column from left), mean differences between the present retrievals and TCCON (“bias”; third column) and standard deviation (“scatter”; last column).

P9L30: For the parameter correlations, I think you should also look at the retrieved aerosol parameters from SWIR-2 when looking at the XCO₂ from SWIR-2. At least check it. I would be surprised if those correlations were not higher than they are for the parameters from the native retrieval, which is VERY different (3 bands, high spectral resolution, etc).

We analyzed correlations of ΔXCO_2 (SWIR-2 - TCCON) with aerosol parameters retrieved from the SWIR-2 configuration. We find that, in comparison to the correlations to the full physics aerosol parameters we used previously,

- correlation with N_{par} changes from -0.05 (FP aerosol parameters) to -0.21 (SWIR-2 aerosol parameters)
- correlation with z_{par} changes from -0.32 (FP aerosol parameters) to 0.05 (SWIR-2 aerosol parameters)
- correlation with α_{par} changes from 0.08 (FP aerosol parameters) to 0.29 (SWIR-2 aerosol parameters)

As the reviewer argued, it does make a difference which aerosol parameters are used here. Interestingly, the SWIR-2 XCO_2 error with respect to TCCON correlates more strongly with particle amount and size in case of the SWIR-2 aerosol retrieval than for the FP aerosol parameters. Scattering layer height, however, correlates less with retrieval errors when the SWIR-2 layer height is used.

Section 4: You should state the purpose of the extensive comparison of the modified SWIR-1 and SWIR-2 retrievals to the native GOSAT retrievals. You take the native GOSAT retrievals as the reference, but they are NOT truth. So the value of several of the Figures (7-11) is dubious. You could shorten the paper by removing some of these figures, since you honestly do not know, in many instances, whether the low-resolution, single band retrievals are actually less accurate than the high-resolution, 3-band retrievals.

The native GOSAT retrievals were shown to compare better to TCCON than the coarse resolution SWIR retrievals in section 3. Of course, the native-GOSAT XCO_2 data are not perfect, but at least they have been shown to be useful in many studies of GOSAT measurements. For this reason, we illustrate retrieval errors with respect to the native GOSAT retrieval (e.g. Figs 7,9,10,11). We do believe it is helpful to show these plots as they give insight into SWIR retrieval errors caused by geophysical dependencies on a global scale. A comparison to TCCON is limited to the site locations of the network and does not reflect variations in geophysical parameters that are observed globally. These plots also help to demonstrate limitations of the proposed sensor. At the same time they help to make the point that our coarse resolution approach is generally comparable to the native RemoTeC GOSAT XCO_2 product.

P11/Fig 7: What are the R (or R^2) values for SWIR-1 and SWIR-2

vs. Native? These are useful to see as well. I suggest also including these numbers in Fig. 9, and perhaps the corresponding main text as well. I.e, is 90% of the variance explained, or 50%? Etc.

We have included Pearson's correlation coefficient in the plots. For both, SWIR-1 and SWIR-2, the value is 0.90.

P17/Fig 12: Per the discussion of the SNR, this relates to my general comment above, about whether the SNRs you actually ran tests on are even remotely achievable. In practice, most instrument builders will tell you that there is a trade off between SNR and spectral resolution. They are not independent, as this work seems to imply. This should be stated more clearly. As I said above, my preference would be to consult with instrument builders and find out what are reasonable noise models for the type of instrument you want to build, and actually run retrieval tests on those, rather than on the likely unrealistic SNR values within this work.

As we discuss in the introduction of the paper, several authors have proposed pursuing a coarse spectral resolution spectrometer for the detection of localized CO₂ and CH₄ emissions from space (e.g. Dennison et al. (2013), Thorpe et al. (2016)). In light of these previous studies, we investigate here whether a CO₂ satellite monitoring mission would be generally within the realms of possibility and which spectral resolutions are favorable. Instrument design is currently in progress and will be the subject of a forthcoming paper. From a technical point of view, the instrument will require a large telescope (e.g. 15 cm diameter) and a fast optics (f-number < 2.5).

References

Dennison, P. E., Thorpe, A. K., Pardyjak, E. R., Roberts, D. A., Qi, Y., Green, R. O., Bradley, E. S., and Funk, C. C.: High spatial resolution mapping of elevated atmospheric carbon dioxide using airborne imaging spectroscopy: Radiative transfer modeling and power plant plume detection, *Remote Sensing of Environment*, 139, 116 – 129, <https://doi.org/https://doi.org/10.1016/j.rse.2013.08.001>, 2013

Thorpe, A. K., Frankenberg, C., Green, R. O., Thompson, D. R., Aubrey, A. D., Mouroulis, P., Eastwood, M. L., and Matheou, G.: The Airborne Methane

Plume Spectrometer (AMPS): Quantitative imaging of methane plumes in real time, in: IEEE Aerospace Conference Proceedings, Vol. 2016 – June, <https://doi.org/10.1109/AERO.2016.7500756>, 2016

List of Relevant Changes

Page 1, line 11:

added “single-band”

Page 3, line 2 – 3:

added “The CO2M mission currently under investigation at the European Space Agency aims at ground resolution of 4 km² (Sierk et al. 2019, Wu et al. 2019a).”

Page 3, line 6:

added “ $\frac{\lambda}{\Delta\lambda} > 6,000$ for CO2M’s SWIR-2 band and”

Page 4, line 8 – 9:

added “Recently, Wu et al. (2019b) showed that at OCO’s native resolving power of $> 20,000$ a single-band retrieval configuration results in almost unchanged XCO₂ retrieval accuracy and precision.”

Page 5, line 8:

added “Due to computational costs, we ...”

Page 5, line 20 – 23:

added “Our approach essentially relates to conditions under which the detector noise is negligible as typical for GOSAT. Under such conditions, other sources of error can be addressed e.g. through evaluating geophysical parameter correlations (section 3 and 4). A forthcoming study will discuss noise performance and retrieval simulations for a hypothetical instrument design.”

Page 5, line 27 – 28:

added “– throughout this work $X_{molecule}$ refers to the column-averaged dry-air mole fraction of a molecule”

Page 6, line 8 – 9:

added “This approach, which is essentially a transmittance calculation along the geometric lightpath, is hereafter referred to as non-scattering retrieval.”

Page 7, line 2 – 3:

removed “(not shown here)” and added “... and results in worse XCO₂ retrieval performance than under the non-scattering assumption”

Page 7, line 9 – 10:

added “Although variations in DFS may lead to changes in the ability of the retrieval algorithm to converge towards the minimum of the cost function, more ...”

Page 7, line 23 – 28:

added “For both, native GOSAT and degraded SWIR configurations, airmass information is derived from ECMWF surface pressure reanalyses (ERA-Interim) and topographic data from the Shuttle Radar Tomography Mission (SRTM). For each sounding, we use ECMWF and SRTM data to calculate the ground-pixel average surface pressure and the corresponding dry airmass. This is the standard operation procedure for RemoTeC trace gas retrievals from the GOSAT, OCO-2 and TROPOMI satellite instruments. Errors in the calculation of the airmass can be caused by erroneous satellite pointing; these errors are part of the overall errors reported for the TCCON validation sites (section 3).”

Page 8, line 1:

added “(i.e. cross sections of the 2.01 μm band need to be scaled by 0.981)”

Page 8, line 30:

added “both Galli et al. (2014) and Wu et al. (2019a)”

Figure 4:

updated Figure shows FP, SWIR-1 and SWIR-2 retrieval standard deviations with respect to TCCON side-by-side.

Page 10, line 2 – 4:

added “Figure 5 also shows XCO₂ retrieval standard deviations per TCCON station. The corresponding data for retrieval performance at individual sites can be found in the supplementary materials.”

Figure 5:

Added three more panels to the plot showing scatter around TCCON. Marker size now reflects number of individual soundings available at each TCCON site.

Page 10, line 19:

added “($\tau=0.1$, $z_{par}=3000$ m, $\alpha_{par}=3.5$)”

Page 10, line 21 – page 11, line 3:

added “An investigation of the impact of the aerosol priors on retrieval perfor-

mance showed that SWIR-2 XCO₂ is only moderately sensitive to the aerosol priors. For instance, varying aerosol prior optical depth by a factor of two or one half results in small changes in standard deviations around TCCON (+0.22 ppm and -0.08 ppm, respectively). Changing scattering layer height priors to $z_{par}=1000$ m or $z_{par}=5000$ m increased scatter around TCCON by +0.04 ppm and +0.43 ppm, respectively. Similarly, scatter around TCCON changes by +0.22 ppm and -0.05 ppm if α_{par} is set to 3.0 and 5.0, respectively.”

In the caption of Figure 5:

added “Comparison of retrieval performances at individual TCCON stations sorted north to south. Marker size indicates amount of colocated soundings at each station. [...] Right: Scatter around TCCON per station for the native, SWIR-1, and SWIR-2 retrievals. Vertical lines mark the average standard deviations (native: 2.43 ppm, SWIR-1: 3.00 ppm, SWIR-2: 3.28 ppm).”

Page 12, line 5:

added “..., while correlation coefficients are 0.90 for both SWIR configurations’.”

Figure 7:

Inserted correlation coefficients in the lower right corners of both panels.

In the caption of Figure 7:

added “Correlation coefficients are displayed in the lower right corners.”

Page 17, line 17:

added “..., such as the one recently proposed by Hasekamp et al. (2019), ...”

Page 17, line 30:

added “Surface reflectance has been shown to be a central driver in methane retrieval precision by Cusworth et al. (2019).”

Page 18, line 4 – 7:

added “Additionally, the SWIR-2 seems better suited for the construction of a cloud filter, because its CO₂ bands have very different optical depths. Similar to the cloud filter currently in use for GOSAT measurements, one could retrieve XCO₂ from the two SWIR-2 bands individually and filter for discrepancies. This scheme should be tested in the future.”

Page 18, line 8 – 9:

added “A forthcoming study addressing these aspects of the proposed sensor is currently under preparation.”

Figure 12:

Introduced a new color scale

Spectral Sizing of a Coarse Spectral Resolution Satellite Sensor for XCO₂

Jonas Simon Wilzewski^{1,2}, Anke Roiger¹, Johan Strandgren¹, Jochen Landgraf³, Dietrich G. Feist^{4,1,5},
Voltaire A. Velasco⁶, Nicholas M. Deutscher⁶, Isamu Morino⁷, Hirofumi Ohyama⁷, Yao Té⁸,
Rigel Kivi⁹, Thorsten Warneke¹⁰, Justus Notholt¹⁰, Manvendra Dubey¹¹, Ralf Sussmann¹²,
Markus Rettinger¹², Frank Hase¹³, Kei Shiomi¹⁴, and André Butz¹⁵

¹Deutsches Zentrum für Luft- und Raumfahrt, Institut für Physik der Atmosphäre, Oberpfaffenhofen, Germany

²Meteorological Institute Munich, Ludwigs-Maximilians-Universität, Munich, Germany

³Netherlands Institute for Space Research, Utrecht, Netherlands

⁴Ludwig-Maximilians-Universität München, Lehrstuhl für Physik der Atmosphäre, Munich, Germany

⁵Max Planck Institute for Biogeochemistry, Jena, Germany

⁶Centre for Atmospheric Chemistry, School of Earth, Atmospheric and Life Sciences, University of Wollongong, NSW, Australia

⁷National Institute for Environmental Studies (NIES), Tsukuba, Japan

⁸LERMA-IPSL, Sorbonne Université, CNRS, Observatoire de Paris, Université PSL, 75005, Paris, France

⁹Finnish Meteorological Institute, FMI, Sodankylä, Finland

¹⁰Institute of Environmental Physics, University of Bremen, Bremen, Germany

¹¹Earth System Observations, Los Alamos National Laboratory, Los Alamos, NM 87545, USA

¹²Karlsruhe Institute of Technology, IMK-IFU, Garmisch-Partenkirchen, Germany

¹³Karlsruhe Institute of Technology, IMK-ASF, Karlsruhe, Germany

¹⁴Japan Aerospace Exploration Agency, Tsukuba, Japan

¹⁵Institute of Environmental Physics, University of Heidelberg, Heidelberg, Germany

Correspondence: Jonas Wilzewski (jonas.wilzewski@dlr.de)

Abstract.

Verifying anthropogenic carbon dioxide (CO₂) emissions globally is essential to inform about the progress of institutional efforts to mitigate man-made climate forcing. To monitor localized emission sources, spectroscopic satellite sensors have been proposed that operate on the CO₂ absorption bands in the shortwave-infrared (SWIR) spectral range with ground resolution as fine as a few tens to about a hundred meters. When designing such sensors, fine ground resolution requires a trade-off towards coarse spectral resolution in order to achieve sufficient noise performance. Since fine ground resolution also implies limited ground coverage, such sensors are envisioned to fly in fleets of satellites, requiring low-cost and simple design, e.g. by restricting the spectrometer to a single spectral band.

Here, we use measurements of the Greenhouse Gases Observing Satellite (GOSAT) to evaluate the spectral resolution and spectral band selection of a prospective satellite sensor with fine ground resolution. To this end, we degrade GOSAT SWIR spectra of the CO₂ bands at 1.6 (SWIR-1) and 2.0 μm (SWIR-2) to coarse spectral resolution, and we evaluate [single-band](#) retrievals of the column-averaged dry-air mole-fractions of CO₂ (XCO₂) by comparison to ground-truth provided by the Total Carbon Column Observing Network (TCCON) and by comparison to global “native” GOSAT retrievals with native spectral resolution and spectral band selection. Coarsening spectral resolution from GOSAT’s native resolving power of >20,000 to

the range of 700 to a few thousand makes the scatter of differences between the SWIR-1 and SWIR-2 retrievals and TCCON increase moderately. For resolving powers of 1,600 (SWIR-1) and 1,200 (SWIR-2), the scatter increases from 2.4 ppm (native) to 3.0 ppm for SWIR-1 and 3.3 ppm for SWIR-2. Coarser spectral resolution yields only marginally worse performance than the native GOSAT configuration in terms of station-to-station variability and geophysical parameter correlations for the TCCON-GOSAT differences. Comparing the SWIR-1 and SWIR-2 configurations to native GOSAT retrievals on the global scale, however, reveals that the coarse resolution SWIR-1 and SWIR-2 configurations suffer from some spurious correlations with geophysical parameters that characterize the light-scattering properties of the scene such as particle amount, size, height and surface albedo. Overall, the SWIR-1 and SWIR-2 configurations with resolving powers of 1,600 and 1,200 show promising performance for future sensor design in terms of random error sources while residual errors induced by light-scattering along the lightpath need to be investigated further. Due to the stronger CO₂ absorption bands in SWIR-2 than in SWIR-1, the former has the advantage that measurement noise propagates less into the retrieved XCO₂ and that some retrieval information on particle scattering properties is accessible.

Copyright statement. To be included by Copernicus

1 Introduction

Accurate and spatiotemporally densely resolved information on localized carbon dioxide (CO₂) emission sources such as power plants is crucial to inform about CO₂ emission reduction targets that national, regional, and municipal administrations worldwide have committed to through their climate action plans. Satellite remote sensing of the column-averaged dry-air mole fractions of CO₂ (XCO₂) could contribute to providing such crucial information if satellite design succeeds in combining fine ground resolution with sufficient precision and if satellite concepts are simple enough to allow for a fleet of sensors enabling broad coverage of the globe.

Global XCO₂ concentration measurements from space were pioneered by the SCIAMACHY mission (e.g. Burrows et al., 1995; Reuter et al., 2010; Schneising et al., 2013) with ground resolution of $\sim 60 \times 30$ km² (Bovensmann et al., 1999). Finer ground resolution (with sparse sampling, though) was subsequently achieved by the Greenhouse Gases Observing Satellite (GOSAT, 10.5 km diameter ground footprint) (Kuze et al., 2009, 2016) and the Orbiting Carbon Observatory (OCO-2, 1.3 \times 2.3 km² ground footprint) (Crisp et al., 2008, 2017). The Chinese TanSat mission has also embarked on this strategy (Yang et al., 2018). GOSAT and OCO-2 offer insights into the natural processes of the carbon cycle (Guerlet et al., 2013a; Parazoo et al., 2013; Liu et al., 2017; Chatterjee et al., 2017) as well as into anthropogenic emission patterns (Hakkarainen et al., 2016). Urban carbon dioxide signals have been detected by these instruments, for example in the Los Angeles basin (Kort et al., 2012; Eldering et al., 2017; Schwandner et al., 2017). Nassar et al. (2017) have demonstrated the ability of OCO-2 to observe anthropogenic CO₂ emissions from individual, coal-fired power plants showcasing the added value of imaging information. A similar concept has been put forward by the CarbonSat mission (Bovensmann et al., 2010), which has evolved

into a candidate for a future European carbon monitoring mission (e.g. Pillai et al., 2016; Broquet et al., 2018; Reuter et al., 2019). [The CO2M mission currently under investigation at the European Space Agency aims at ground resolution of 4 km² \(Sierk et al., 2019; Wu et al., 2019a\)](#). All these satellite missions and concepts rely on a multi-band spectral configuration that covers the oxygen (O₂) A-band at roughly 0.76 μm (NIR), and the CO₂ bands at 1.6 (SWIR-1) and 2.0 μm (SWIR-2). The spectral resolution ranges from resolving powers $\frac{\lambda}{\Delta\lambda} > 20,000$ (with λ the wavelength and $\Delta\lambda$ the full-width-half-maximum of the instrument spectral response function) for GOSAT, OCO-2, and Tansat to [6,000 for CO2M's SWIR-2 band and 4,000 for CarbonSat's SWIR-2 band](#). The typical XCO₂ native GOSAT retrievals attempt to make use of these bands by retrieving XCO₂ simultaneously with atmospheric scattering properties.

For methane (CH₄), which poses similar remote sensing challenges as CO₂, it has been demonstrated that a satellite spectrometer operating at coarse spectral resolution ($\frac{\lambda}{\Delta\lambda}$ of a few hundred) on a single absorption band (around 2.35 μm) can achieve successful CH₄ hot-spot detection with a ground resolution of 30 m (Thompson et al., 2016). Similar results for CH₄ have been reported from aircraft sensors that reach ground pixel sizes on the order of 1-10 m (Dennison et al., 2013; Thorpe et al., 2016a, b; Krings et al., 2018). Dennison et al. (2013) suggested that measuring the 2.0 μm CO₂ bands with a spectral resolution of 10 nm ($\frac{\lambda}{\Delta\lambda} \approx 200$) enables a space-borne spectrometer design that results in ground resolutions as fine as 60×60 m². Thorpe et al. (2016a) have shown that their airborne AVIRIS-NG instrument exploiting the CO₂ absorption bands at 2.0 μm at a spectral resolution of roughly 5 nm ($\frac{\lambda}{\Delta\lambda} \approx 400$) enables quantitative retrievals of CO₂ in localized emission plumes. Thorpe et al. (2016b) suggested that, for CH₄, a spectrometer design with a spectral resolution of 1 nm ($\frac{\lambda}{\Delta\lambda} \approx 2,000$) could provide an optimal trade-off that allows for accurate CH₄ quantification while supporting small ground pixels.

This study is motivated by the margins that coarse spectral resolution offers with respect to improving ground resolution and that single-band configurations offer with respect to deploying a fleet of several low-cost satellites. Fig. 1 schematically illustrates the key advantage of an assumed 50×50 m² ground resolution spectrometer over an instrument with km-scale resolution for point-source observation. If the localized source plume does not fill the satellite's entire ground pixel, the XCO₂ enhancement averages with the background concentration field over the satellite pixel. For the example in Fig. 1, this leads to a maximum of 3 ppm enhancement for a satellite sensor with 2×2 km² ground resolution. Shrinking the ground pixels leads to larger enhancements in the vicinity of the source, simply because the plume fills a larger portion of the (smaller) pixels. In Fig. 1, 50×50 m² ground resolution delivers 12 ppm enhancement at 2 km downwind distance, plus a sampling of the plume cross-section by more than 10 pixels. Further downwind, where the plume has laterally spread to the km-scale, enhancements per pixel are similar for fine and coarse ground resolution, but the fine ground resolution sensor would still sample the plume by multiple ground pixels. Thus, a sensor with fine ground resolution allows for less stringent precision requirements (per ground pixel), and it could potentially resolve plume shapes at some detail. Since small ground pixels imply less backscattered photons, sensor design for fine ground resolution typically needs to compensate by enhancing light throughput of the spectrometer and by collecting more photons in the spectral domain, e.g. by coarsening spectral resolution. Since finer ground resolution implies narrower ground coverage for the same detector size, global monitoring with fine ground resolution almost certainly implies the need for a fleet of sensors which would be easier to realize if the sensors had a simple, single-band configuration instead of full spectral coverage from the NIR into SWIR-2.

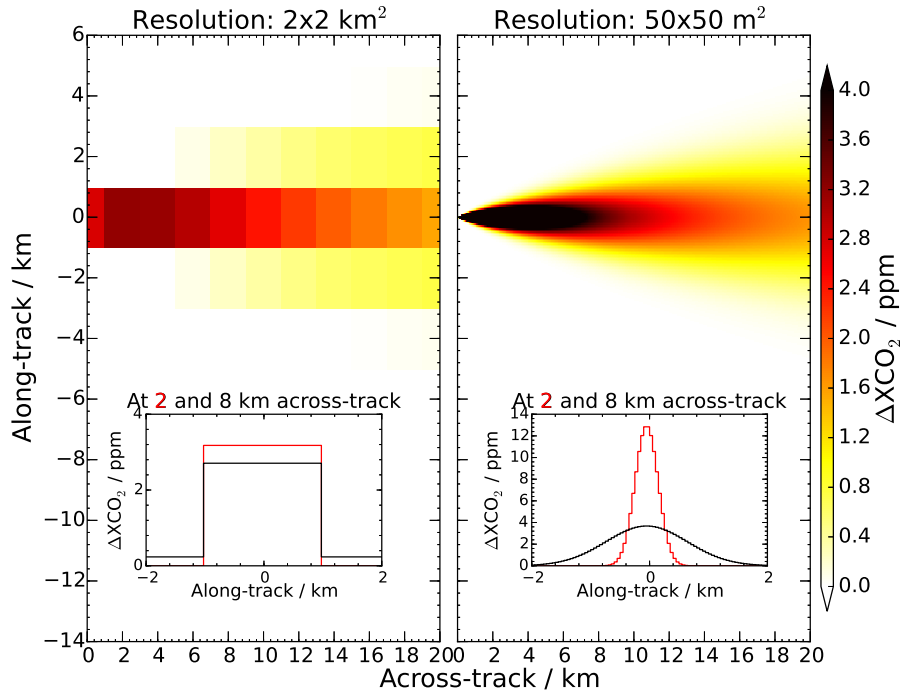


Figure 1. Schematic Gaussian plume of the XCO₂ enhancement (ΔXCO_2) originating from a power plant with $12.3 \text{ Mt CO}_2 \text{ y}^{-1}$ emission rate (wind from left to right, Guifford-Pasquill stability class C; power plant at the origin; satellite assumed to move from bottom to top, sampling left to right) as seen (without noise) by hypothetical satellite spectrometers with $2 \times 2 \text{ km}^2$ ground pixels (left), and with $50 \times 50 \text{ m}^2$ ground pixels (right). Insets show ΔXCO_2 measured by the sensors at 2 km (red) and 8 km (black) downwind of the source along the plume cross section (note different ΔXCO_2 scales in insets).

Here, we aim at evaluating the performance of a hypothetical XCO₂ sensor that has coarse spectral resolution in a single-band configuration. That is, we evaluate a sensor concept which measures the CO₂ bands near either 1.6 (SWIR-1) or 2.0 μm (SWIR-2) with resolving power in the range of 700 to a few thousand, i.e. roughly between the AVIRIS-NG and CarbonSat concepts. Galli et al. (2014) conducted a related study where they spectrally degraded GOSAT soundings to resolutions ranging from native GOSAT resolution down to $\frac{\lambda}{\Delta\lambda} \approx 3,000$ while leaving the multi-band configuration (NIR, SWIR-1, SWIR-2) of the XCO₂ retrievals untouched. They found that coarser spectral resolution typically implies larger statistical and systematic XCO₂ errors when compared to ground truth. Galli et al. (2014), however, did not address the range of resolving powers and the single-band selection covered here. [Recently, Wu et al. \(2019b\) showed that at OCO's native resolving power of \$> 20,000\$ a single-band retrieval configuration results in almost unchanged XCO₂ retrieval accuracy and precision.](#)

Section 2 explains our methodological approach that spectrally degrades GOSAT measurements of the SWIR-1 or SWIR-2 bands to coarser spectral resolution. In section 3, we assess retrieval performance for the SWIR-1 and SWIR-2 configurations for various resolving powers by comparing our results to ground-truth from the Total Carbon Column Observing Network

(TCCON). Thereby, we derive a target spectral resolution for which we carry out a global evaluation with respect to native GOSAT measurements in section 4. Section 5 discusses and concludes on the findings.

2 Methodology

GOSAT measures spectra of backscattered solar radiation in three spectral bands centered on the O₂ A-band (NIR), the relatively weak CO₂ and CH₄ bands in the vicinity of 1.6 μm (SWIR-1), and the strong CO₂ and water vapor (H₂O) bands around 2.0 μm (SWIR-2). GOSAT’s thermal infrared band recording telluric emission spectra is not used here. We use the level 1B (L1B) data version 201.202, and we add the two measured polarization directions to represent the backscattered radiances. **We** [Due to computational costs, we](#) restrict our analysis to cloud-free, quality screened soundings over land as identified by the native GOSAT retrievals of the RemoTeC algorithm (Butz et al., 2011) within the Climate Change Initiative of the European Space Agency (ESA) (Buchwitz et al., 2017), available for download at <http://www.esa-ghg-cci.org>. In total, the set comprises 469,689 L1B spectra in the period from April 1, 2009 to December 31, 2016. A typical GOSAT spectrum together with the coarse resolution variants discussed below is shown in Fig. 2.

A key advantage of GOSAT measurements over other CO₂ missions, such as OCO-2, is the wide spectral coverage in SWIR-1 and SWIR-2. The broad spectral coverage allows for conveniently sizing the retrieval windows without being limited by the actual bandpass of the spectrometer. In particular, GOSAT’s SWIR-1 and SWIR-2 bands cover, respectively, two and three rotational-vibrational absorption bands of CO₂. In order to mimic a coarse resolution sensor, we convolve the native GOSAT L1B spectra by a Gaussian function of selectable full-width-at-half-maximum (FWHM). Since we want to isolate the effects of spectral resolution and spectral band selection, we do not add extra noise to the convolved spectra. One would expect extra noise when going to smaller ground pixels as we envision for a future sensor. Estimating the extra noise, however, would require a detailed instrument model which is not available here. [Our approach essentially relates to conditions under which the detector noise is negligible as typical for GOSAT. Under such conditions, other sources of error can be addressed e.g. through evaluating geophysical parameter correlations \(section 3 and 4\). A forthcoming study will discuss noise performance and retrieval simulations for a hypothetical instrument design.](#) Figure 2 illustrates the spectral convolution approach for a hypothetical spectral resolving power of 1,200 (blue line) and 1,600 (red line) in SWIR-1 and SWIR-2, respectively, in comparison to native GOSAT spectra. We assume that the proposed sensor will have a detector with 256 spectral pixels.

The native and degraded GOSAT measurements are submitted to the RemoTeC retrieval algorithm (Butz et al., 2009, 2011; Guerlet et al., 2013b), which is in routine use for retrieving XCO₂ (and XCH₄ – [throughout this work Xmolecule refers to the column-averaged dry-air mole fraction of a molecule](#)) from GOSAT (Buchwitz et al., 2017), XCO₂ from OCO-2 (Wu et al., 2018) and XCH₄ from Sentinel-5 Precursor/TROPOMI (Hu et al., 2018). For GOSAT measurements with native spectral resolution, we deploy RemoTeC in its full-physics (“native” GOSAT) mode, i.e. RemoTeC uses four spectral windows within the NIR, SWIR-1 and SWIR-2 ranges (see Table 1 and Fig. 2) and retrieves XCO₂, XCH₄ together with three particle scattering parameters and other parameters such as surface albedo and spectral shifts. The three particle parameters are the total column number density N_{par} , the center height z_{par} of a Gaussian height distribution and the power α_{par} of a power-law size dis-

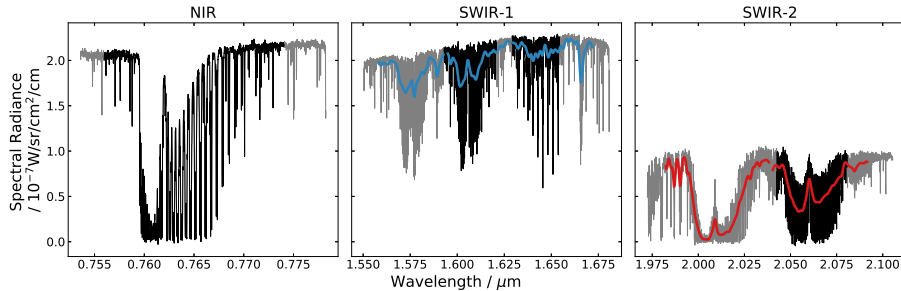


Figure 2. Measured GOSAT spectrum of the backscattered radiance in the NIR, SWIR-1 and SWIR-2 (left to right) ranges shown in grey with respective GOSAT retrieval windows in bold black. The spectrally degraded measurements at resolving powers of $\sim 1,200$ (SWIR-1) and $\sim 1,600$ (SWIR-2) are shown in bold blue and bold red respectively.

tribution $n(r) \sim r^{-\alpha_{par}}$ with particle radius r . The native GOSAT configuration is equivalent to the standard retrieval also in operation for ESA’s climate change initiative (e.g. Buchwitz et al. (2017)).

		Coarse spectral resolution sensor		native GOSAT
		SWIR-1	SWIR-2	
Spectral Windows Used / nm		1.559 - 1.593		0.7741 - 0.7560
		1.595 - 1.628		1.593 - 1.621
		1.630 - 1.672		1.629 - 1.654
			1.982 - 2.038	
			2.040 - 2.092	2.042 - 2.081
FWHM / cm^{-1}	0.75 ... 5.1 ... 8.0	0.75 ... 3.1 ... 7.0	0.24	
FWHM / nm	0.20 ... 1.37 ... 2.15	0.31 ... 1.29 ... 2.90	0.1	
approx. Resolving Power	8,100 ... 1,200 ... 760	6,500 ... 1,600 ... 700	> 20,000	

Table 1. Spectral windows for the various retrieval configurations. Bold numbers indicate the spectral resolution that was chosen for subsequent analyses (see section 3).

For degraded spectral resolution, we use either SWIR-1 or SWIR-2 alone (see Table 1), from which we retrieve XCO₂ (as well as XCH₄ in SWIR-1) and auxiliary surface albedo and spectral shift parameters. The spectral degradation of the modeled spectra to coarse resolution follows the same approach as for the measurements. First, RemoTeC calculates spectra for GOSAT’s native spectral resolution, then the convolution with a Gaussian function simulates the hypothetical measurements at coarse spectral resolution. For degraded spectral resolution, the SWIR-1 retrievals also adjust XH₂O and XCH₄, but neglect scattering by particles (Rayleigh scattering is included) and thus, no particle scattering parameters are retrieved. [This approach, which is essentially a transmittance calculation along the geometric lightpath, is hereafter referred to as non-scattering retrieval.](#)

Sensitivity studies have shown that retrieving atmospheric scattering parameters from the individual CO₂ bands at coarse spectral resolution in the SWIR-1 band suffers from low information content (~~not shown here~~)[and results in worse XCO₂ retrieval performance than under the non-scattering assumption.](#) In the SWIR-2, we retrieve XH₂O along with XCO₂. Employing the standard RemoTeC Phillips-Tikhonov (e.g. Butz et al., 2012) regularization, we additionally retrieve our standard three
5 particle parameters from SWIR-2. We found a regularization strength that allows for retrieving an average of 0.38 degrees of freedom (DFS) for particles (DFS \gtrsim 1.5 are typically found in native GOSAT retrievals). Despite this low DFS, the performance of the retrieval was significantly improved in comparison to a non-scattering retrieval. As the spectral resolution coarsens, the average degrees of freedom for particles decrease from 0.45 (at 6,500 resolving power) to 0.32 (at 700 resolving power). ~~More~~
[Although variations in DFS may lead to changes in the ability of the retrieval algorithm to converge towards the minimum of the cost function, more](#) than 75 % of all retrievals converge at any given FWHM that we consider in this study. We note
10 that while we divide the SWIR-1 and SWIR-2 retrievals into several sub-windows, the retrieved XCO₂ is coupled among the sub-windows.

The actual spectral retrieval windows are defined in Table 1 and illustrated in Fig. 2. The spectral boundaries of the retrieval windows are identical at all selected FWHM. For the coarse spectral resolution SWIR setups, we have chosen to cover two
15 CO₂ absorption bands each, while the native GOSAT retrievals cover only one of the bands in SWIR-1 and one of the bands in SWIR-2. Our choice of spectral retrieval windows maximizes the information on CO₂ for the coarse resolution retrievals. However, a fine-tuning of the spectral windows for the proposed sensor may be conducted in a future study with an instrument noise model at hand. For native GOSAT resolution, the two extra bands would provide mostly redundant information while adding significant computational cost. Further, the coarse spectral resolution configurations cover (almost) transparent ranges
20 in the vicinity of the absorption bands in order to constrain surface albedo, even at coarse spectral resolution. If the spectral boundaries of the retrieval windows lie within the CO₂ absorption bands, i.e. parts of the CO₂ absorption bands are “cut-off”, this loss of information generally leads to poorer retrieval performance with respect to TCCON (not shown here).

[For both, native GOSAT and degraded SWIR configurations, airmass information is derived from ECMWF surface pressure reanalyses \(ERA-Interim\) and topographic data from the Shuttle Radar Tomography Mission \(SRTM\). For each sounding, we use ECMWF and SRTM data to calculate the ground-pixel average surface pressure and the corresponding dry airmass. This is the standard operation procedure for RemoTeC trace gas retrievals from the GOSAT, OCO-2 and TROPOMI satellite instruments. Errors in the calculation of the airmass can be caused by erroneous satellite pointing; these errors are part of the overall errors reported for the TCCON validation sites \(section 3\).](#)

Butz et al. (2013) have shown that the CO₂ absorption cross sections used in RemoTeC for the SWIR-1 bands and the
30 CO₂ band centered at 2.06 μ m in SWIR-2 are consistent to within 0.16 % while the band centered at 2.01 μ m in SWIR-2 is inconsistent with its neighboring SWIR-2 band. Since Butz et al. (2013) used a shorter measurement period than here, we repeat that study for our period and, we determine a scaling factor for the absorption cross sections at 2.01 μ m with respect to the 2.06 μ m band. To this end, we select ocean-glint scenes that are confidently free of cloud and aerosol using the “upper-edge” method (Butz et al., 2013). Then, we run RemoTeC retrievals on the 2.01 μ m and the 2.06 μ m bands separately under
35 the non-scattering assumption. The average ratio of the retrieved XCO₂ is our scaling factor, which amounts to ~~1.856 %~~ [0.981](#)

at native GOSAT spectral resolution ~~-(i.e. cross sections of the 2.01 μm band need to be scaled by 0.981)~~. The “upper-edge” method is also used to adjust the scaling factor at each spectral degradation to reflect the impact of the convolution procedure on the low resolution spectra. The updated factors differ on the sub-permil level from the correction at native spectral resolution.

3 Validation with the TCCON Network

5 As detailed in section 2, we run XCO₂ retrievals for the native GOSAT configuration, and for the coarse spectral resolution SWIR configurations on a global set of cloud-free GOSAT measurements. The SWIR-1 and SWIR-2 configurations are run for various spectral resolutions, i.e. for various values of the FWHM of the Gaussian function that convolves the native GOSAT spectra. The native GOSAT configuration serves as the reference run corresponding to state-of-the-art full-physics retrievals from a spectrometer with fine spectral resolution and wide spectral coverage (from NIR to SWIR-2). The SWIR-1 and SWIR-2
10 configurations represent our test cases for a potential future sensor with coarse spectral resolution and single-band spectral coverage. To evaluate our retrievals, we compare retrieved XCO₂ with measurements by the ground-based TCCON network (Wunch et al., 2011a, b; Messerschmidt et al., 2011; Kiel et al., 2019) (the stations we do not use could not be colocated with satellite measurements of our GOSAT dataset). We use data from 24 TCCON stations worldwide from the “GGG2014” dataset (available at <https://tccodata.org>). GOSAT soundings are defined to be coincident with a TCCON station if the satellite
15 sounding is located within 5° with respect to latitude/longitude of the respective ground station. The GOSAT XCO₂ retrieval is then compared to the average of the TCCON XCO₂ measurements within ± 2 hours of the GOSAT sounding time.

XCO₂ precision is commonly quantified through the standard deviation of the differences (“scatter”) between GOSAT and TCCON. Figure 3 shows that, while coarser spectral resolution implies larger scatter overall, there is some margin for the choice of spectral resolution in the SWIR-1 band and the figure suggests that the scatter around TCCON exhibits a “plateau”
20 in resolving power space just beyond the critical spectral resolution necessary to distinguish between two typical adjacent CO₂ absorption lines in the SWIR-1 (the critical resolving powers are $\sim 3,300$ in SWIR-1 and $\sim 2,700$ in SWIR-2). This resolving power is marked by the dotted line in Fig. 3. As spectral lines are blended into a broader spectral shape by our convolution procedure, the non-scattering SWIR-1 retrieval retains a very similar scatter around TCCON for another 1,000 resolving powers. This pattern is not observed for SWIR-2 scatter around TCCON, which gradually increases towards lower resolving
25 powers (bold red line in Fig. 3). We also conducted a sensitivity study where we switched off the retrieval of particle scattering properties in SWIR-2, i.e. using the same non-scattering configuration in SWIR-2 as in SWIR-1. Then, the scatter of SWIR-2 with respect to around TCCON increases significantly (faint red line in Fig. 3) indicating that while DFS for the particle retrievals is small, XCO₂ retrievals benefit. Our observation that spectral resolution degradation for the SWIR-1 and SWIR-2 configurations generally results in larger scatter (than for the native GOSAT retrievals) is in broad agreement with the tendency
30 reported in ~~Galli et al. (2014)~~ both Galli et al. (2014) and Wu et al. (2019a) who, however, did not assess the resolution range reported here.

To constrain the resolving power of our future satellite sensor, the scatter around TCCON is the most crucial variable, since the sensor will be built to study local scale XCO₂ enhancements. As a consequence, spectral resolving powers greater than

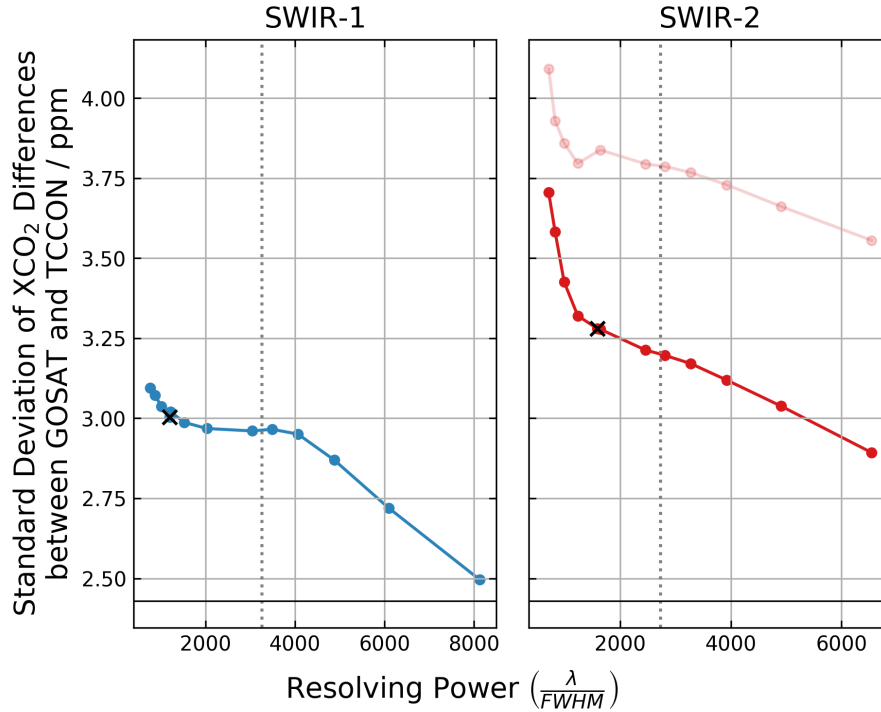


Figure 3. Standard deviation of retrieved XCO₂ values in SWIR-1 (left) and SWIR-2 (right) around TCCON measurements plotted as a function of resolving power. For SWIR-2, the faint line indicates scatter for a non-scattering retrieval. The dotted line marks the resolving power at which spectral lines become indistinguishable in the convolved spectra. The black horizontal line indicates the native GOSAT scatter around TCCON. The \times marks the resolving power that we study in the rest of the article.

the ones that lead to a steep increase in scatter around TCCON in Fig. 3 seem reasonable choices. A technical constraint for the spectral resolution for the envisioned satellite sensor is that the target spectral range ought to be imaged entirely onto the presumed 256 spectral pixels of the sensor’s detector assuming a sampling ratio of three. Thereby we define two target resolving powers of 1,200 and 1,600 in SWIR-1 and SWIR-2 (marked with \times in Fig. 3). For these choices, Figure 4 shows the correlation of the SWIR-1, SWIR-2, and native GOSAT XCO₂ retrievals with TCCON. The standard deviations around TCCON amount to 2.43 ppm (native), 3.00 ppm (SWIR-1) and 3.28 ppm (SWIR-2). Given that all retrievals here are without bias correction, the three configurations yield different mean differences (“biases”) with respect to TCCON. Generally, although spectral resolution degradation causes a change of the overall bias, a overall bias itself is irrelevant for emission estimates which rely on concentration gradients. Even if the satellite data are to be used in combination with other CO₂ measurements, it is common practice to derive a scaling factor of the satellite retrievals with respect to ground-truth.

Figure 5 resolves the biases per TCCON station for the resolving powers of 1,200 and 1,600 in SWIR-1 and SWIR-2, respectively. Typically, the standard deviation among these station-by-station biases (“bias variability”) is taken as a measure for regional systematic errors which cause regional-scale spurious gradients and thus, they are detrimental for regional assessment

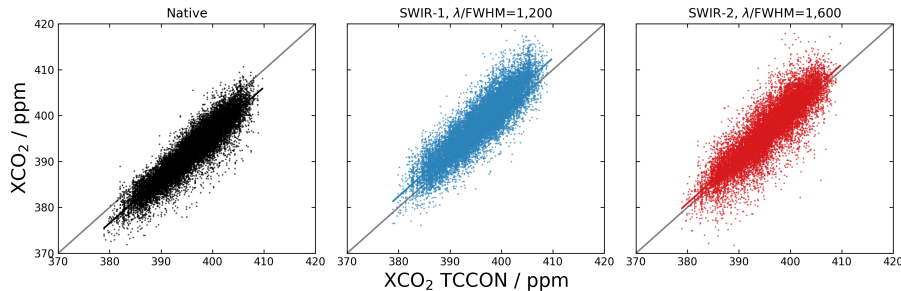


Figure 4. Correlation between XCO_2 retrieved from GOSAT with the TCCON network. **BlackLeft:** native GOSAT retrieval; **BlueCenter:** SWIR-1 retrieval at 1,200 resolving power; **RedRight:** SWIR-2 retrieval at 1,600 resolving power. The grey line indicates a 1:1 correlation line; the colored lines show linear fits to the respective dataset. Standard deviations around TCCON amount to 2.43 ppm (native, compare e.g. Guerlet et al. (2013b)), 3.00 ppm (SWIR-1) and 3.28 ppm (SWIR-2).

of sources and sinks. The present retrieval configurations lead to marginally increased TCCON bias variability from 0.94 ppm for native GOSAT up to 0.99 ppm and 0.97 ppm in SWIR-1 and SWIR-2 retrievals, respectively. [Figure 5 also shows \$XCO_2\$ retrieval standard deviations per TCCON station. The corresponding data for retrieval performance at individual sites can be found in the supplementary materials.](#) Regional scale variability of our proposed retrievals is not of utmost importance as our goal is to make consistent measurements on a local scale. To this end, correlations of retrieval errors caused by parameters that vary on local scales are more informing.

For diagnosing spurious dependencies of the retrieved XCO_2 on locally variable geophysical parameters, we examine parameter correlations of the GOSAT-TCCON differences. Fig. 6 shows correlations of the native GOSAT, SWIR-1 (resolving power: 1,200) and SWIR-2 (resolving power: 1,600) retrievals for surface albedo (at $0.774 \mu\text{m}$ for native GOSAT, at $1.600 \mu\text{m}$ for SWIR-1, at $2.099 \mu\text{m}$ for SWIR-2), the scattering optical thickness (SOT) and the three particle parameters N_{par} , z_{par} , and α_{par} characterizing particle number density, particle layer height and particle size. The particle parameters are taken from native GOSAT runs since SWIR-1 does not retrieve the parameters and SWIR-2 retrievals exhibit little DFS. The GOSAT-TCCON departures show a small correlation ($R > 0.1$) with surface albedo for both SWIR-1 and native GOSAT configurations, while the SWIR-2 retrievals do not show any correlation. Since the SWIR-1 configuration neglects particle scattering, it appears reasonable that the GOSAT-TCCON departures correlate with albedo which mediates the importance of scattering with respect to the direct lightpath. Yet, only small correlations are found for SWIR-1 errors with SOT, particle layer height and particle size ($R < 0.1$). Minor SWIR-1 error correlations with respect to particle number density ($R = 0.11$) are present around TCCON stations. For SWIR-2, the correlation with the particle layer height shows $R < -0.3$. Although we do account for scattering in the SWIR-2, the strong regularization of the retrieval leads to convergence close to the a priori ($\tau = 0.1$, $z_{par} = 3000 \text{ m}$, $\alpha_{par} = 3.5$) of the particle parameters. Therefore, it is not surprising that correlations still exist with particle scattering properties also in SWIR-2. [An investigation of the impact of the aerosol priors on retrieval performance showed that SWIR-2 \$XCO_2\$ is only moderately sensitive to the aerosol priors. For instance, varying aerosol prior optical depth by a factor of two or one half results](#)

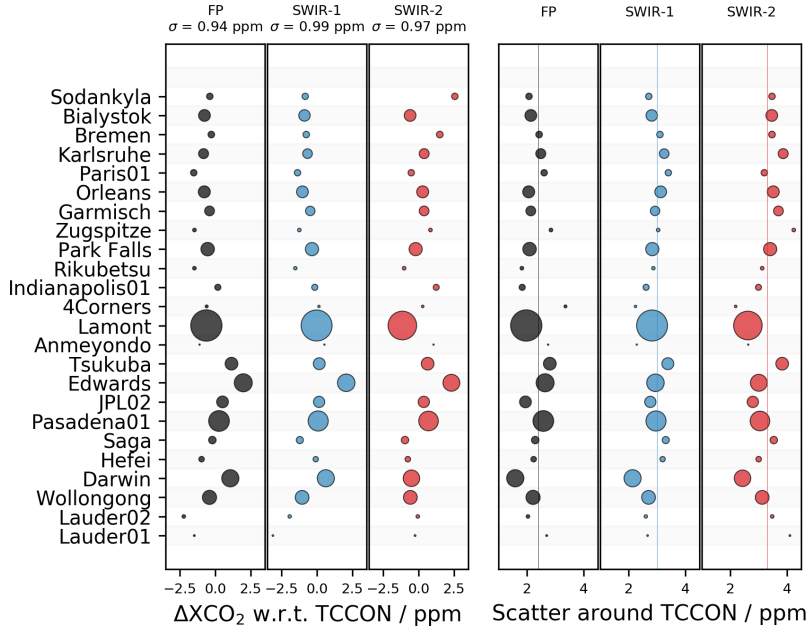


Figure 5. Comparison of retrieval performances at individual TCCON stations sorted north to south. Marker size indicates amount of colocated soundings at each station. Left: Station-by-station mean differences between TCCON and the native (left black), SWIR-1 (middle blue), and SWIR-2 (right red) retrievals from GOSAT. TCCON stations are sorted north to south. The standard deviation of mean differences among the stations, σ , amounts to 0.94 ppm (native), 0.99 ppm (SWIR-1) and 0.97 ppm (SWIR-2). Right: Scatter around TCCON per station for the native, SWIR-1, and SWIR-2 retrievals. Vertical lines mark the average standard deviations (native: 2.43 ppm, SWIR-1: 3.00 ppm, SWIR-2: 3.28 ppm).

in small changes in standard deviations around TCCON (+0.22 ppm and -0.08 ppm, respectively). Changing scattering layer height priors to $z_{par}=1000$ m or $z_{par}=5000$ m increased scatter around TCCON by +0.04 ppm and +0.43 ppm, respectively. Similarly, scatter around TCCON changes by +0.22 ppm and -0.05 ppm if α_{par} is set to 3.0 and 5.0, respectively. SWIR-2 retrieval errors around TCCON sites do not significantly correlate with SOT, particle number density and the size parameter.

- 5 Native GOSAT retrievals consistently show small correlations with all particle parameters. In addition (not shown), correlations with $|R| > 0.1$ are observed for SWIR-1 (and not for SWIR-2) with other geophysical variables like slant airmass of the geometric lightpath ($R=-0.17$) and water vapor column ($R=0.21$).

4 Global Evaluation with Native GOSAT Retrievals

For evaluation on the global scale, we take XCO_2 from native GOSAT retrievals as the reference. The SWIR-1 and SWIR-2 retrievals are discussed for resolving powers of 1,200 and 1,600, respectively. We subtract the overall biases found by the

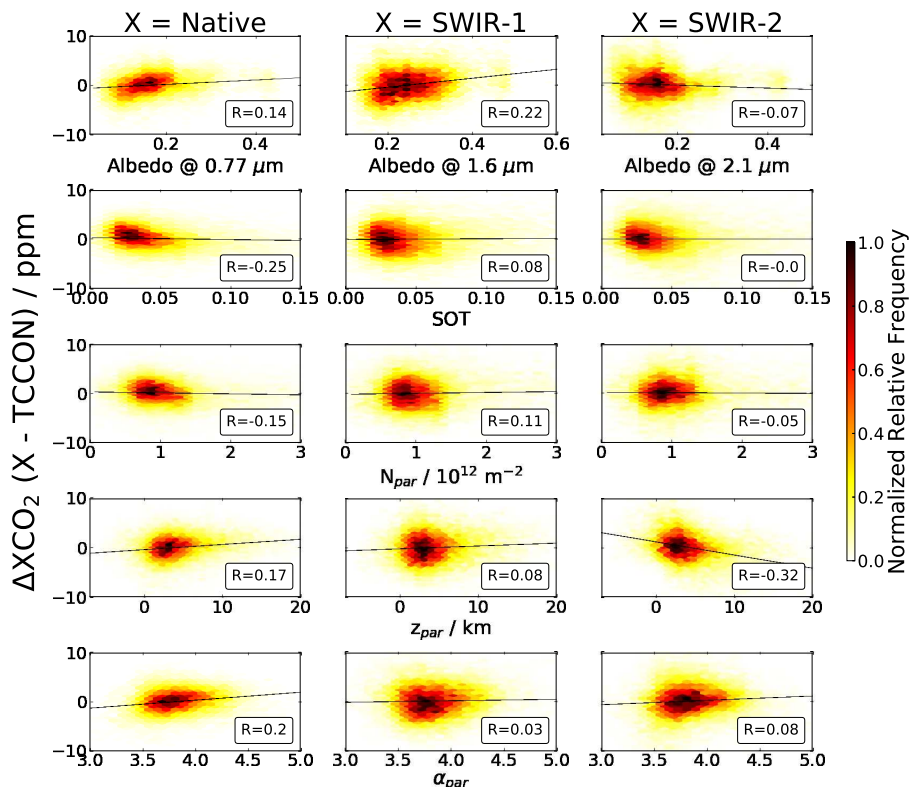


Figure 6. Differences between TCCON and native GOSAT (left), SWIR-1 (middle) and SWIR-2 (right) for selected geophysical parameters. Pearson’s correlation coefficient R is shown in the corner of each subplot. The solid line is a linear fit to the data. Color encodes relative occurrence of data points.

TCCON analysis from all XCO₂ retrievals discussed here (-3.6 ppm, 2.49 ppm and 1.04 ppm for the native, SWIR-1 and SWIR-2 configurations, respectively).

Fig. 7 shows the correlations of the SWIR-1 and SWIR-2 configurations with the native GOSAT retrievals. The standard deviations of the differences to native GOSAT (“scatter”) amount to 2.85 ppm and 2.69 ppm for SWIR-1 and SWIR-2, respectively, while correlation coefficients are 0.90 for both SWIR configurations. Although the overall biases with respect to TCCON have been subtracted, the global analysis (containing many more data than the TCCON analysis) yields non-vanishing mean differences (“bias”) of 0.59 ppm for SWIR-1 and -0.29 ppm for SWIR-2 with respect to native GOSAT, presumably as a consequence of an uneven distribution of TCCON sites around the globe. Figure 8 resolves bias and scatter of the SWIR configurations in geographic latitude and season. Figure 8 (upper panels) illustrates that SWIR-1 bias and scatter are both enhanced in the northern hemisphere. Averaging all seasons, SWIR-1 bias and scatter peak at 1.93 ppm and 3.34 ppm, respectively, between 20 and 30° N where the planet’s large deserts are located. Deserts imply bright surfaces and desert dust aerosols which may impact the SWIR-1 retrievals configured under the non-scattering assumption. For the SWIR-2 configuration, fig-

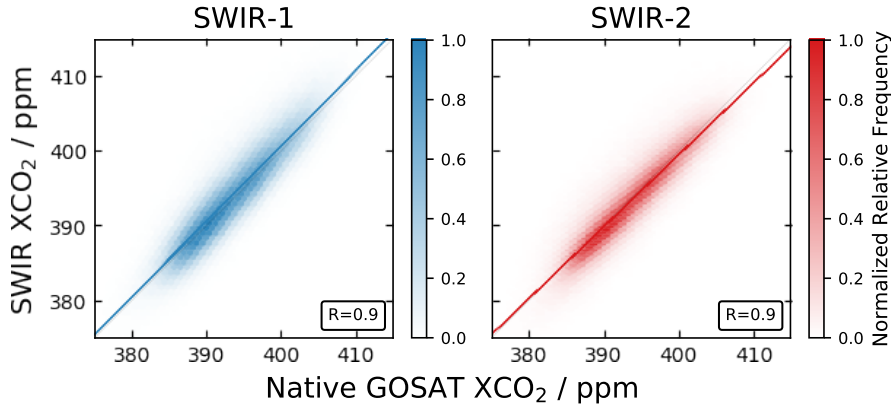


Figure 7. Retrieved SWIR-1 (left) and SWIR-2 (right) XCO₂ plotted versus the corresponding native GOSAT retrievals. The colored lines indicate linear fits to the data, the grey line marks the 1:1 correlation. Scatter amounts to 2.85 ppm and to 2.69 ppm in SWIR-1 and SWIR-2, respectively. [Correlation coefficients are displayed in the lower right corners.](#) Color shading encodes relative occurrence of data points.

ure 8 (lower panels) shows a meridional gradient for scatter and an unclear pattern for bias. Average SWIR-2 scatter varies between 2.03 ppm (at 15° S) and 3.20 ppm (at 65° N). The bias seems to indicate that SWIR-2 retrievals underestimate native GOSAT over the desert latitudes (20° N) and overestimate in higher latitudes (60° N). Seasonal variations generally follow the annual average patterns and no clear seasonal dependencies are detectable. Figures 9 and 10 show maps of the differences between the native GOSAT configuration and SWIR-1 and SWIR-2 averaged on $1 \times 1^\circ$ for the full record of eight years of GOSAT observations (2009-2016). The global maps retrace the general observations of the zonal averages shown in Fig. 8. SWIR-1 overestimates native GOSAT retrievals throughout the high albedo regions of the Sahara, central Asia, and tentatively in central Australia. SWIR-2 tends to overestimate native GOSAT in the high latitudes and in Amazonia. Over the deserts the patterns are mixed.

Fig. 11 examines correlations of the retrieval differences with selected geophysical parameters similar to the analysis undertaken for TCCON (section 3, Fig. 6). Among various parameters tested, most significant correlations are found for the geophysical parameters that control the scattering regime. These parameters are surface albedo, SOT, number density of scatterers (N_{par}), center height of the scattering layer (z_{par}), the power-law parameter for the scattering particle size distribution (α_{par}). As in Fig. 6, particle scattering parameters are taken from the native GOSAT retrievals. Generally, the SWIR-1 and SWIR-2 retrievals show parameter correlations which are more significant on the global scale than what has been found for the TCCON evaluation. The correlation coefficients R are typically on the order of 0.2-0.3 and peak at 0.5 for the correlation of the SWIR-2 bias with the number density of scatterers N_{par} . This is true for the SWIR-2 retrievals although the configuration allows for some freedom fitting the particle parameters (DFS=0.38 on average). We also tried a non-scattering variant for SWIR-2 (not shown) which yielded clearly inferior performance (see also figure 3) due to correlations with other parameters such as the water vapor column and the slant airmass.

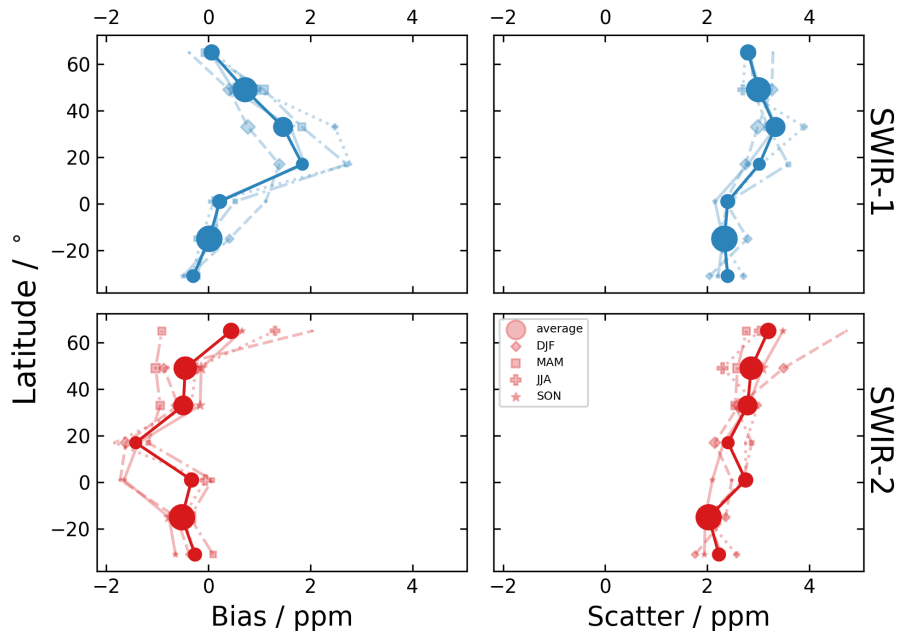


Figure 8. Retrieval bias (left) and scatter (right) with respect to native GOSAT XCO₂ over land as a function of latitude for the SWIR-1 (top) and SWIR-2 retrievals (bottom) in 16° bins. Bold circles indicate the average bias and scatter, while seasonal variations are shown for boreal winter (DJF, diamonds), spring (MAM, squares), summer (JJA, plus) and fall (SON, stars). Symbol size indicates the relative number of GOSAT observations over land in the respective latitudinal bin.

5 Discussion and conclusions

We have evaluated the performance of XCO₂ retrievals from solar backscatter satellite observations for a hypothetical sensor that operates at moderate spectral resolution in either the SWIR-1 (around 1.6 μm) or the SWIR-2 band (around 2.0 μm). Both configurations, SWIR-1 and SWIR-2, cover tens of CO₂ absorption lines and the selected retrieval windows all cover transparent regions toward the shortwave and the longwave ends to constrain surface albedo and its spectral variation. The absorption optical depths in SWIR-1, however, are generally less than those in SWIR-2. SWIR-1, in addition to CO₂, covers a CH₄ absorption band, both configurations have interfering water vapor absorption. For SWIR-2, we implemented a retrieval variant of the RemoTeC algorithm that allows for estimating three parameters that characterize light scattering in terms of amount, size and height of the scattering particles. Yet, degrees-of-freedom for the particle retrieval amount to only 0.38 on average which indicates that the information content on scattering effects is limited. Nevertheless, our evaluation shows that the highly constrained particle retrieval outperforms a non-scattering retrieval in SWIR-2. For SWIR-1, information content on particle scattering was found even less and therefore, the SWIR-1 configuration is based on the non-scattering assumption. Performance was evaluated by mimicking the SWIR-1 and SWIR-2 sensors using spectrally degraded GOSAT observations

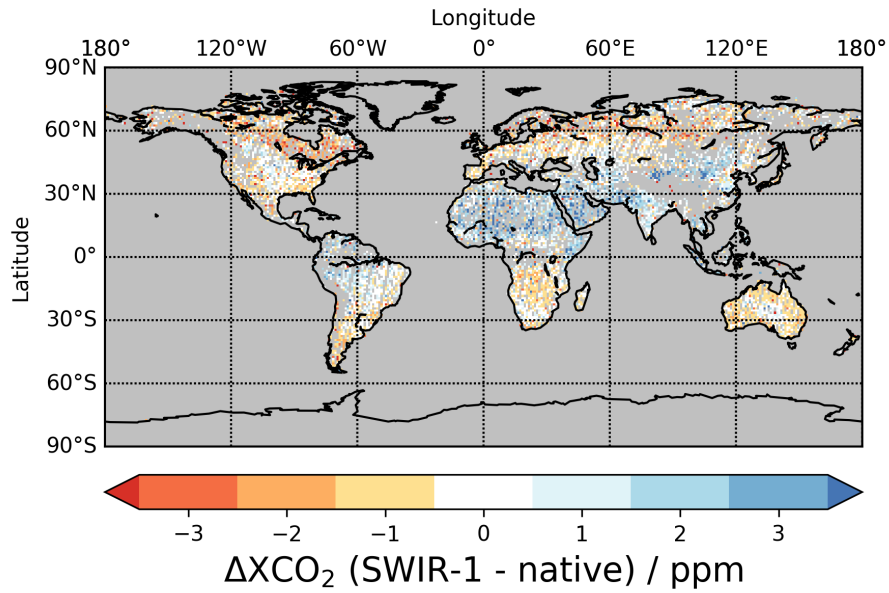


Figure 9. Differences between native GOSAT and SWIR-1 retrievals averaged on $1 \times 1 \times 1^\circ$ for eight years of GOSAT observations. A global mean bias of 0.45 ppm was subtracted from the graph.

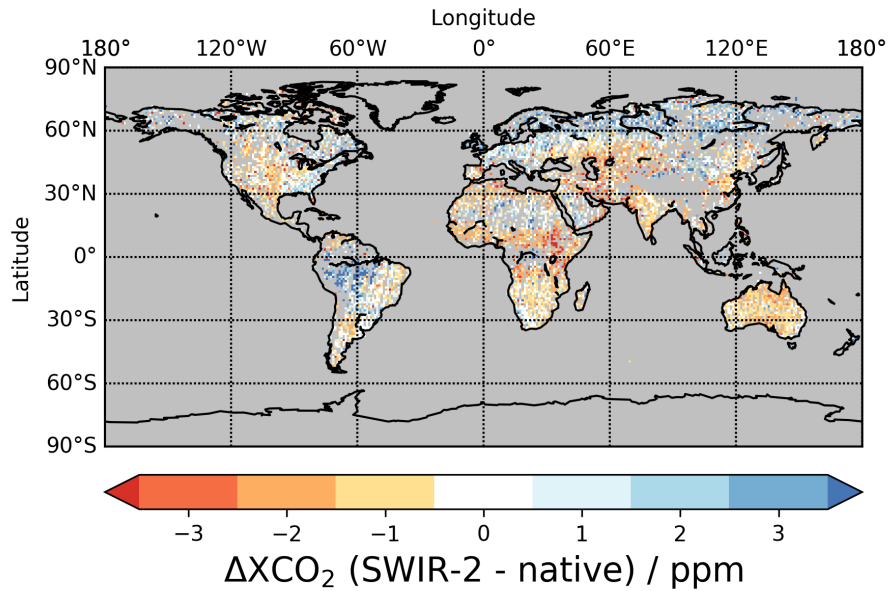


Figure 10. Differences between native GOSAT and SWIR-2 retrievals averaged on $1 \times 1 \times 1^\circ$ for eight years of GOSAT observations. A global mean bias of 0.03 ppm was subtracted from the graph.

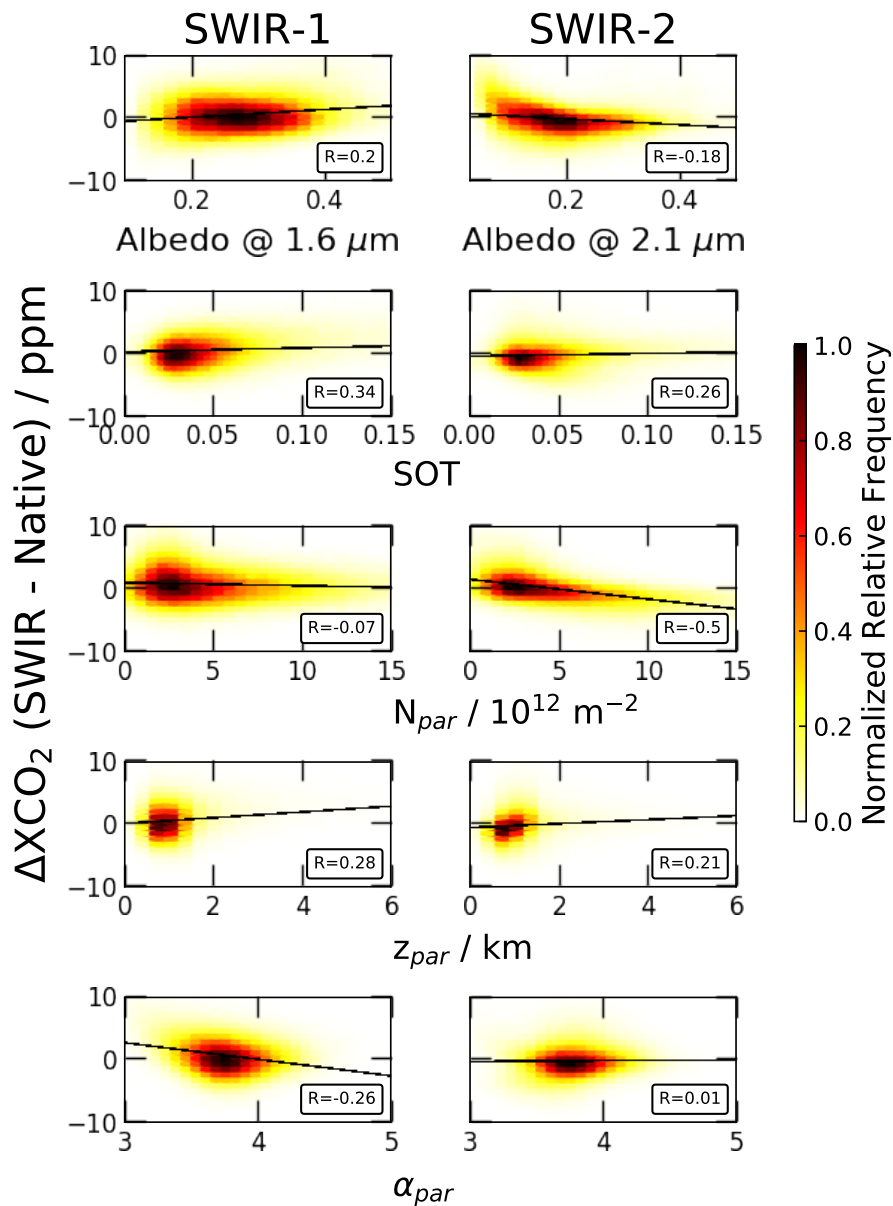


Figure 11. Differences between native GOSAT and the SWIR-1 (left) and SWIR-2 (right) configurations for selected geophysical parameters. Pearson's correlation coefficient R is shown in the corner of each subplot. The solid line is a linear fit to the data. Color encodes relative occurrence of data points.

for the years 2009 to 2016, which allowed for comparisons with ground-truth provided by TCCON and for comparisons with the native GOSAT retrievals (based on GOSAT's full spectral resolution and spectral band coverage).

Comparing the SWIR-1 and SWIR-2 retrievals to TCCON, we tried various resolving powers between 8,100 and 760 for SWIR-1 and 6,500 and 700 for SWIR-2 which is the range roughly in-between the CarbonSat concept and hyperspectral imagers such as AVIRIS-NG. Generally, the scatter with respect to TCCON increases moderately with decreasing resolving power. For SWIR-2, we find ~~an~~ a relatively sharp increase below resolving power 1,000. The standard configurations that we have chosen for further analyses correspond to resolving powers of 1,200 and 1,600 for SWIR-1 and SWIR-2, respectively. The corresponding scatter around TCCON amounts to 3.00 ppm and 3.28 ppm, respectively, while native GOSAT retrievals scatter by 2.43 ppm. These ~~standard~~ configurations fit on a detector with 256 spectral pixels assuming a sampling ratio of 3 per FWHM. Other evaluation metrics such as the overall global bias and the station-by-station biases do not show significantly worse performance than the native GOSAT configuration for the TCCON comparisons. Likewise, correlations with the scattering parameters are mostly small for the TCCON coincidences. The evaluation using the native GOSAT retrievals on the global scale shows differences in the range of 2 to 3 ppm, which, for SWIR-1, clearly correlate with desert areas. In contrast to the TCCON evaluation, the differences to native GOSAT for both, SWIR-1 and SWIR-2, also correlate with particle scattering parameters (R typically in the range 0.2-0.3, up to 0.5). Thus, assuming that the native GOSAT retrievals are more accurate, we expect the SWIR-1 and SWIR-2 configurations to suffer from regionally correlated errors due to particle scattering. Possibly, an additional aerosol sensor, such as the one recently proposed by Hasekamp et al. (2019), may help to overcome challenges in scenes with difficult aerosol loads.

Our goal is to assess the suitability of the spectral sizing of the SWIR-1 and SWIR-2 configurations for a hypothetical sensor that maps localized CO₂ sources with high spatial resolution. Our study indicates that limiting band coverage to a single SWIR band and operating at a spectral resolving power between 6,000 and 1,000 does not substantially degrade XCO₂ retrieval performance in terms of errors that appear random in our comparisons to TCCON and to the native GOSAT retrievals. However, the SWIR-1 and SWIR-2 configurations are less capable of accounting for particle scattering effects than the configurations of the type of the native GOSAT design. The hypothetical sensor aims at discriminating plumes from background concentration fields on the scale of hundreds of meters to a few kilometers with a ground resolution on the order of $50 \times 50 \text{ m}^2$ enabling enhanced contrast in the vicinity of the sources (Fig. 1). Thus, in terms of random errors, our findings are promising for using one of our SWIR-1 and SWIR-2 configurations. For the errors induced by particle scattering, the implications largely depend on whether the scattering regime can be assumed homogeneous on the respective scales of hundreds of meters to a few kilometers. Even if atmospheric scattering properties are homogeneous, ground albedo varies substantially on these scales. Surface reflectance has been shown to be a central driver in methane retrieval precision by Cusworth et al. (2019). However, ground albedo is presumably more temporally consistent than aerosols, for example, and so could be more easily defined by independent measurements.

Our study isolates the effects of spectral resolution and spectral band selection, but it postpones the assessment whether sufficient signal-to-noise is achievable. While our evaluation reveals no clear preference for SWIR-1 or SWIR-2, we expect that the assessment of signal-to-noise will favor the SWIR-2 configuration. Fig. 12 shows the noise error of the XCO₂ retrievals

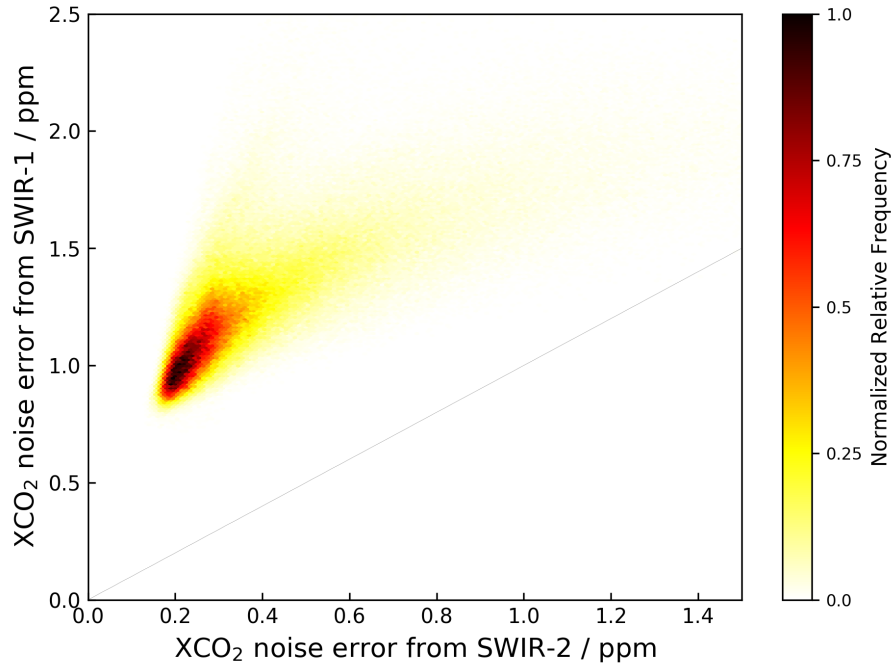


Figure 12. XCO₂ noise errors for SWIR-1 (ordinate) and SWIR-2 (abscissa). The grey line indicates the 1:1 correlation. Color shading encodes the relative occurrence of data points.

from SWIR-1 and SWIR-2. These errors are calculated by Gaussian error propagation of GOSAT's radiance noise through the RemoTeC algorithm. Propagated noise errors in SWIR-2 are on average a factor 2.9 less than those in SWIR-1 which is largely due to SWIR-2 covering the stronger CO₂ absorption bands. Thus, we expect that achieving the required signal-to-noise is less demanding for SWIR-2 than for SWIR-1. [Additionally, the SWIR-2 seems better suited for the construction of a cloud filter,](#)

- 5 [because its CO₂ bands have very different optical depths. Similar to the cloud filter currently in use for GOSAT measurements, one could retrieve XCO₂ from the two SWIR-2 bands individually and filter for discrepancies. This scheme should be tested in the future.](#) Overall, we recommend further studies to consolidate the SWIR-2 configuration in terms of instrument design and noise performance and to evaluate the relevance of scattering induced errors for the targeted fine spatial resolution. [A forthcoming study addressing these aspects of the proposed sensor is currently under preparation.](#)

TCCON station	Citation	TCCON station	Citation
Sodankyla	Kivi et al. (2014)	Lamont	Wennberg et al. (2016b)
Bialystok	Deutscher et al. (2015)	Anmeyondo	Goo et al. (2014)
Bremen	Notholt et al. (2014)	Tsukuba	Morino et al. (2018a)
Karlsruhe	Hase et al. (2015)	Edwards	Iraci et al. (2016a)
Paris	Té et al. (2014)	JPL	Wennberg et al. (2016a)
Orleans	Warneke et al. (2014)	Pasadena	Wennberg et al. (2015)
Garmisch	Sussmann and Rettinger (2018a)	Saga	Kawakami et al. (2014)
Zugspitze	Sussmann and Rettinger (2018b)	Hefei	Liu et al. (2018)
Park Falls	Wennberg et al. (2017)	Rikubetsu	Morino et al. (2018b)
Izana	Blumenstock et al. (2017)	Ascension Island	Feist et al. (2014)
Indianapolis	Iraci et al. (2016b)	Darwin	Griffith et al. (2014a)
Four Corners	Dubey et al. (2014), Lindenmaier et al. (2014)	Reunion	De Mazière et al. (2017)
Wollongong	Griffith et al. (2014b)	Lauder 1	Sherlock et al. (2014a)
Lauder 2	Sherlock et al. (2014b)		

Data availability.

Table 2. Overview of TCCON datasets used in this work.

Competing interests. The authors declare that they have no conflict of interest.

Disclaimer.

Acknowledgements. We gratefully acknowledge support from DLR VO-R for funding the young investigator research group "Greenhouse Gases". We thank [Luca Bugliaro for valuable feedback on our work. We also thank](#) all TCCON members for making their data available on the TCCON data archive at <https://tccondata.org/>. The Ascension Island TCCON station has been supported by the European Space Agency (ESA) under grant 3-14737 and by the German Bundesministerium für Wirtschaft und Energie (BMWi) under grant 50EE1711C. The TCCON projects for the Rikubetsu and Tsukuba sites are supported in part by the GOSAT series project. The Paris TCCON site has received fundings from Sorbonne Université, the French research center CNRS, the French space agency CNES and Région Île-de-France. We acknowledge funding from ESA, DLR and the EC (projects RINGO and VERIFY) for the TCCON sites Bremen, Orleans and Bialystok.

5
10
Nicholas Deutscher is supported by an Australian Research Council Future Fellowship, FT180100327. [KIT/IMK-ASF \(Karlsruhe\) and KIT/IMK-IFU \(Garmisch-Partenkirchen, in cooperation with University of Augsburg\) acknowledge BMWi for funding data analysis and delivery through DLR projects \(Contracts 50EE1711A, B, C, D\).](#)

References

- Blumenstock, T., Hase, F., Schneider, M., García, O. E., and Sepúlveda, E.: TCCON data from Izana (ES), Release GGG2014.R1, <https://doi.org/10.14291/tccon.ggg2014.izana01.r1>, 2017.
- Bovensmann, H., Burrows, J. P., Buchwitz, M., Frerick, J., Noël, S., Rozanov, V. V., Chance, K. V., and Goede, A. P. H.: SCIAMACHY: Mission Objectives and Measurement Modes, *Journal of the Atmospheric Sciences*, 56, 127–150, [https://doi.org/10.1175/1520-0469\(1999\)056<0127:SMOAMM>2.0.CO;2](https://doi.org/10.1175/1520-0469(1999)056<0127:SMOAMM>2.0.CO;2), 1999.
- Bovensmann, H., Buchwitz, M., Burrows, J. P., Reuter, M., Krings, T., Gerilowski, K., Schneising, O., Heymann, J., Tretner, A., and Erzinger, J.: A remote sensing technique for global monitoring of power plant CO₂ emissions from space and related applications, *Atmospheric Measurement Techniques*, 3, 781–811, <https://doi.org/10.5194/amt-3-781-2010>, 2010.
- 10 Broquet, G., Bron, F. M., Renault, E., Buchwitz, M., Reuter, M., Bovensmann, H., Chevallier, F., Wu, L., and Ciais, P.: The potential of satellite spectro-imagery for monitoring CO₂ emissions from large cities, *Atmospheric Measurement Techniques*, 11, 681–708, <https://doi.org/10.5194/amt-11-681-2018>, 2018.
- Buchwitz, M., Reuter, M., Schneising, O., Hewson, W., Detmers, R., Boesch, H., Hasekamp, O., Aben, I., Bovensmann, H., Burrows, J., Butz, A., Chevallier, F., Dils, B., Frankenberg, C., Heymann, J., Lichtenberg, G., Maziere, M. D., Notholt, J., Parker, R., Warneke, T., Zehner, C., Griffith, D., Deutscher, N., Kuze, A., Suto, H., and Wunch, D.: Global satellite observations of column-averaged carbon dioxide and methane: The GHG-CCI XCO₂ and XCH₄ CRDP3 data set, *Remote Sensing of Environment*, 203, 276 – 295, <https://doi.org/https://doi.org/10.1016/j.rse.2016.12.027>, 2017.
- 15 Burrows, J. P., Hölzle, E., Goede, A. P., Visser, H., and Fricke, W.: SCIAMACHY-scanning imaging absorption spectrometer for atmospheric cartography, *Acta Astronautica*, 35, 445–451, [https://doi.org/10.1016/0094-5765\(94\)00278-T](https://doi.org/10.1016/0094-5765(94)00278-T), 1995.
- 20 Butz, A., Hasekamp, O. P., and Aben, I.: Retrievals of atmospheric CO₂ from simulated space-borne measurements of backscattered near-infrared sunlight: accounting for aerosol effects, *Applied Optics*, 48, 3322–3336, <https://doi.org/10.1364/AO.48.003322>, 2009.
- Butz, A., Guerlet, S., Hasekamp, O., Schepers, D., Galli, A., Aben, I., Frankenberg, C., Hartmann, J.-M., Tran, H., Kuze, A., Keppel-Aleks, G., Toon, G., Wunch, D., Wennberg, P., Deutscher, N., Griffith, D., Macatangay, R., Messerschmidt, J., Notholt, J., and Warneke, T.: Toward accurate CO₂ and CH₄ observations from GOSAT, *Geophysical Research Letters*, 38, L14812, <https://doi.org/10.1029/2011GL047888>, 2011.
- 25 Butz, A., Galli, A., Hasekamp, O., Landgraf, J., Tol, P., and Aben, I.: TROPOMI aboard Sentinel-5 Precursor: Prospective performance of CH₄ retrievals for aerosol and cirrus loaded atmospheres, *Remote Sensing of Environment*, 120, 267–276, <https://doi.org/10.1016/j.rse.2011.05.030>, 2012.
- Butz, A., Guerlet, S., Hasekamp, O. P., Kuze, A., and Suto, H.: Using ocean-glint scattered sunlight as a diagnostic tool for satellite remote sensing of greenhouse gases, *Atmospheric Measurement Techniques*, 6, 2509–2520, <https://doi.org/10.5194/amt-6-2509-2013>, 2013.
- 30 Chatterjee, A., Gierach, M. M., Sutton, A. J., Feely, R. A., Crisp, D., Eldering, A., Gunson, M. R., O'Dell, C. W., Stephens, B. B., and Schimel, D. S.: Influence of El Niño on atmospheric CO₂ over the tropical Pacific Ocean: Findings from NASA's OCO-2 mission, *Science*, 358, <https://doi.org/10.1126/science.aam5776>, 2017.
- Crisp, D., Miller, C. E., and DeCola, P. L.: NASA Orbiting Carbon Observatory: measuring the column averaged carbon dioxide mole fraction from space, *Journal Of Applied Remote Sensing*, 2, 23 508, <https://doi.org/10.1117/1.2898457>, 2008.
- Crisp, D., Pollock, H., Rosenberg, R., Chapsky, L., Lee, R., Oyafuso, F., Frankenberg, C., Dell, C., Bruegge, C., Doran, G., Eldering, A., Fisher, B., Fu, D., Gunson, M., Mandrake, L., Osterman, G., Schwandner, F., Sun, K., Taylor, T., Wennberg, P., and Wunch, D.: The

- on-orbit performance of the Orbiting Carbon Observatory-2 (OCO-2) instrument and its radiometrically calibrated products, *Atmospheric Measurement Techniques*, 10, 59–81, <https://doi.org/10.5194/amt-10-59-2017>, 2017.
- Cusworth, D. H., Jacob, D. J., Varon, D. J., Chan Miller, C., Liu, X., Chance, K., Thorpe, A. K., Duren, R. M., Miller, C. E., Thompson, D. R., Frankenberg, C., Guanter, L., and Randles, C. A.: Potential of next-generation imaging spectrometers to detect and quantify methane point sources from space, *Atmospheric Measurement Techniques Discussions*, 2019, 1–29, <https://doi.org/10.5194/amt-2019-202>, <https://www.atmos-meas-tech-discuss.net/amt-2019-202/>, 2019.
- De Mazière, M., Sha, M. K., Desmet, F., Hermans, C., Scolas, F., Kumps, N., Metzger, J.-M., Dufлот, V., and Cammas, J.-P.: TCCON data from Réunion Island (RE), Release GGG2014.R1, <https://doi.org/10.14291/tccon.ggg2014.reunion01.r1>, 2017.
- Dennison, P. E., Thorpe, A. K., Pardyjak, E. R., Roberts, D. A., Qi, Y., Green, R. O., Bradley, E. S., and Funk, C. C.: High spatial resolution mapping of elevated atmospheric carbon dioxide using airborne imaging spectroscopy: Radiative transfer modeling and power plant plume detection, *Remote Sensing of Environment*, 139, 116 – 129, <https://doi.org/https://doi.org/10.1016/j.rse.2013.08.001>, 2013.
- Deutscher, N. M., Notholt, J., Messerschmidt, J., Weinzierl, C., Warneke, T., Petri, C., and Grupe, P.: TCCON data from Bialystok (PL), Release GGG2014.R1, <https://doi.org/10.14291/tccon.ggg2014.bialystok01.r1/1183984>, 2015.
- Dubey, M. K., Lindenmaier, R., Henderson, B. G., Green, D., Allen, N. T., Roehl, C. M., Blavier, J.-F., Butterfield, Z. T., Love, S., Hamelmann, J. D., and Wunch, D.: TCCON data from Four Corners (US), Release GGG2014.R0, <https://doi.org/10.14291/tccon.ggg2014.fourcorners01.r0/1149272>, 2014.
- Eldering, A., Wennberg, P. O., Crisp, D., Schimel, D. S., Gunson, M. R., Chatterjee, A., Liu, J., Schwandner, F. M., Sun, Y., O’Dell, C. W., Frankenberg, C., Taylor, T., Fisher, B., Osterman, G. B., Wunch, D., Hakkarainen, J., Tamminen, J., and Weir, B.: The Orbiting Carbon Observatory-2 early science investigations of regional carbon dioxide fluxes, *Science*, 358, <https://doi.org/10.1126/science.aam5745>, 2017.
- Feist, D. G., Arnold, S. G., John, N., and Geibel, M. C.: TCCON data from Ascension Island (SH), Release GGG2014.R0, <https://doi.org/10.14291/tccon.ggg2014.ascension01.r0/1149285>, 2014.
- Galli, A., Guerlet, S., Butz, A., Aben, I., Suto, H., Kuze, A., Deutscher, N. M., Notholt, J., Wunch, D., Wennberg, P. O., Griffith, D. W., Hasekamp, O., and Landgraf, J.: The impact of spectral resolution on satellite retrieval accuracy of CO₂ and CH₄, *Atmospheric Measurement Techniques*, 7, 1105–1119, <https://doi.org/10.5194/amt-7-1105-2014>, 2014.
- Goo, T.-Y., Oh, Y.-S., and Velazco, V. A.: TCCON data from Anmeyondo (KR), Release GGG2014.R0, <https://doi.org/10.14291/tccon.ggg2014.anmeyondo01.r0/1149284>, 2014.
- Griffith, D. W., Deutscher, N. M., Velazco, V. A., Wennberg, P. O., Yavin, Y., Keppel-Aleks, G., Washenfelder, R. A., Toon, G. C., Blavier, J.-F., Paton-Walsh, C., Jones, N. B., Kettlewell, G. C., Connor, B. J., Macatangay, R. C., Roehl, C., Ryzek, M., Glowacki, J., Culgan, T., and Bryant, G. W.: TCCON data from Darwin (AU), Release GGG2014.R0, <https://doi.org/10.14291/tccon.ggg2014.darwin01.r0/1149290>, 2014a.
- Griffith, D. W., Velazco, V. A., Deutscher, N. M., Paton-Walsh, C., Jones, N. B., Wilson, S. R., Macatangay, R. C., Kettlewell, G. C., Buchholz, R. R., and Riggensbach, M. O.: TCCON data from Wollongong (AU), Release GGG2014.R0, <https://doi.org/10.14291/tccon.ggg2014.wollongong01.r0/1149291>, 2014b.
- Guerlet, S., Basu, S., Butz, A., Krol, M., Hahne, P., Houweling, S., Hasekamp, O. P., and Aben, I.: Reduced carbon uptake during the 2010 Northern Hemisphere summer from GOSAT, *Geophysical Research Letters*, 40, 2378–2383, <https://doi.org/10.1002/grl.50402>, 2013a.
- Guerlet, S., Butz, A., Schepers, D., Basu, S., Hasekamp, O. P., Kuze, A., Yokota, T., Blavier, J. F., Deutscher, N. M., Griffith, D. W., Hase, F., Kyro, E., Morino, I., Sherlock, V., Sussmann, R., Galli, A., and Aben, I.: Impact of aerosol and thin cirrus on retrieving

- and validating XCO₂ from GOSAT shortwave infrared measurements, *Journal of Geophysical Research Atmospheres*, 118, 4887–4905, <https://doi.org/10.1002/jgrd.50332>, 2013b.
- Hakkarainen, J., Ialongo, I., and Tamminen, J.: Direct space-based observations of anthropogenic CO₂ emission areas from OCO₂, *Geophysical Research Letters*, 43, 400–411, <https://doi.org/10.1002/2016GL070885>, 2016.
- 5 Hase, F., Blumenstock, T., Dohe, S., Groß, J., and Kiel, M.: TCCON data from Karlsruhe (DE), Release GGG2014.R1, <https://doi.org/10.14291/tcon.ggg2014.karlsruhe01.r1/1182416>, 2015.
- Hasekamp, O. P., Fu, G., Rusli, S. P., Wu, L., Noia, A. D., aan de Brugh, J., Landgraf, J., Smit, J. M., Rietjens, J., and van Amerongen, A.: Aerosol measurements by SPEXone on the NASA PACE mission: expected retrieval capabilities, *Journal of Quantitative Spectroscopy and Radiative Transfer*, 227, 170 – 184, <https://doi.org/https://doi.org/10.1016/j.jqsrt.2019.02.006>, <http://www.sciencedirect.com/science/article/pii/S0022407318308653>, 2019.
- 10 Hu, H., Landgraf, J., Detmers, R., Borsdorff, T., Aan de Brugh, J., Aben, I., Butz, A., and Hasekamp, O.: Toward Global Mapping of Methane With TROPOMI: First Results and Intersatellite Comparison to GOSAT, *Geophysical Research Letters*, 45, 3682–3689, <https://doi.org/10.1002/2018GL077259>, 2018.
- Iraci, L. T., Podolske, J. R., Hillyard, P. W., Roehl, C., Wennberg, P. O., Blavier, J.-F., Landeros, J., Allen, N., Wunch, D., Zavaleta, J., Quigley, E., Osterman, G. B., Albertson, R., Dunwoody, K., and Boyden, H.: TCCON data from Edwards (US), Release GGG2014.R1, <https://doi.org/10.14291/tcon.ggg2014.edwards01.r1/1255068>, 2016a.
- 15 Iraci, L. T., Podolske, J. R., Hillyard, P. W., Roehl, C., Wennberg, P. O., Blavier, J.-F., Landeros, J., Allen, N., Wunch, D., Zavaleta, J., Quigley, E., Osterman, G. B., Barrow, E., and Barney, J.: TCCON data from Indianapolis (US), Release GGG2014.R1, <https://doi.org/10.14291/tcon.ggg2014.indianapolis01.r1/1330094>, 2016b.
- 20 Kawakami, S., Ohyama, H., Arai, K., Okumura, H., Taura, C., Fukamachi, T., and Sakashita, M.: TCCON data from Saga (JP), Release GGG2014.R0, <https://doi.org/10.14291/tcon.ggg2014.saga01.r0/1149283>, 2014.
- Kiel, M., O’Dell, C. W., Fisher, B., Eldering, A., Nassar, R., MacDonald, C. G., and Wennberg, P. O.: How bias correction goes wrong: measurement of XCO₂ affected by erroneous surface pressure estimates, *Atmospheric Measurement Techniques*, 12, 2241–2259, <https://doi.org/10.5194/amt-12-2241-2019>, 2019.
- 25 Kivi, R., Heikkinen, P., and Kyrö, E.: TCCON data from Sodankylä (FI), Release GGG2014.R0, <https://doi.org/10.14291/tcon.ggg2014.sodankyla01.r0/1149280>, 2014.
- Kort, E. A., Frankenberg, C., Miller, C. E., and Oda, T.: Space-based observations of megacity carbon dioxide, *Geophysical Research Letters*, 39, <https://doi.org/10.1029/2012GL052738>, 2012.
- Krings, T., Neininger, B., Gerilowski, K., Krautwurst, S., Buchwitz, M., Burrows, J. P., Lindemann, C., Ruutz, T., Schüttemeyer, D., and Bovensmann, H.: Airborne remote sensing and in situ measurements of atmospheric CO₂ to quantify point source emissions, *Atmospheric Measurement Techniques*, 11, 721–739, <https://doi.org/10.5194/amt-11-721-2018>, 2018.
- 30 Kuze, A., Suto, H., Nakajima, M., and Hamazaki, T.: Thermal and near infrared sensor for carbon observation Fourier-transform spectrometer on the Greenhouse Gases Observing Satellite for greenhouse gases monitoring, *Applied Optics*, 48, 6716, <https://doi.org/10.1364/AO.48.006716>, 2009.
- 35 Kuze, A., Suto, H., Shiomi, K., Kawakami, S., Tanaka, M., Ueda, Y., Deguchi, A., Yoshida, J., Yamamoto, Y., Kataoka, F., Taylor, T. E., and Buijs, H. L.: Update on GOSAT TANSO-FTS performance, operations, and data products after more than 6 years in space, *Atmospheric Measurement Techniques*, 9, 2445–2461, <https://doi.org/10.5194/amt-9-2445-2016>, 2016.

- Lindenmaier, R., Dubey, M. K., Henderson, B. G., Butterfield, Z. T., Herman, J. R., Rahn, T., and Lee, S.-H.: Multiscale observations of CO₂, 13CO₂, and pollutants at Four Corners for emission verification and attribution, *Proceedings of the National Academy of Sciences*, 111, 8386–8391, <https://doi.org/10.1073/pnas.1321883111>, <https://www.pnas.org/content/111/23/8386>, 2014.
- 5 Liu, C., Wang, W., Sun, Y., and ,: TCCON data from Hefei (PRC), Release GGG2014.R0, <https://doi.org/10.14291/tcon.ggg2014.hefei01.r0>, 2018.
- Liu, J., Bowman, K. W., Schimel, D. S., Parazoo, N. C., Jiang, Z., Lee, M., Bloom, A. A., Wunch, D., Frankenberg, C., Sun, Y., O'Dell, C. W., Gurney, K. R., Menemenlis, D., Gierach, M., Crisp, D., and Eldering, A.: Contrasting carbon cycle responses of the tropical continents to the 2015–2016 El Niño, *Science*, 358, <https://doi.org/10.1126/science.aam5690>, 2017.
- 10 Messerschmidt, J., Geibel, M. C., Blumenstock, T., Chen, H., Deutscher, N. M., Engel, A., Feist, D. G., Gerbig, C., Gisi, M., Hase, F., Katrynski, K., Kolle, O., Lavrič, J. V., Notholt, J., Palm, M., Ramonet, M., Rettinger, M., Schmidt, M., Sussmann, R., Toon, G. C., Truong, F., Warneke, T., Wennberg, P. O., Wunch, D., and Xueref-Remy, I.: Calibration of TCCON column-averaged CO₂: the first aircraft campaign over European TCCON sites, *Atmospheric Chemistry and Physics*, 11, 10765–10777, <https://doi.org/10.5194/acp-11-10765-2011>, 2011.
- Morino, I., Matsuzaki, T., and Horikawa, M.: TCCON data from Tsukuba (JP), 125HR, Release GGG2014.R2, <https://doi.org/10.14291/tcon.ggg2014.tsukuba02.r2>, 2018a.
- 15 Morino, I., Yokozeki, N., Matsuzaki, T., and Horikawa, M.: TCCON data from Rikubetsu (JP), Release GGG2014.R2, <https://doi.org/10.14291/tcon.ggg2014.rikubetsu01.r2>, 2018b.
- Nassar, R., Hill, T. G., McLinden, C. A., Wunch, D., Jones, D. B. A., and Crisp, D.: Quantifying CO₂ emissions from individual power plants from space, *Geophysical Research Letters*, 44, 10,045–10,053, <https://doi.org/10.1002/2017GL074702>, 2017.
- 20 Notholt, J., Petri, C., Warneke, T., Deutscher, N. M., Palm, M., Buschmann, M., Weinzierl, C., Macatangay, R. C., and Grupe, P.: TCCON data from Bremen (DE), Release GGG2014.R0, <https://doi.org/10.14291/tcon.ggg2014.bremen01.r0/1149275>, 2014.
- Parazoo, N. C., Bowman, K., Frankenberg, C., Lee, J. E., Fisher, J. B., Worden, J., Jones, D. B., Berry, J., Collatz, G. J., Baker, I. T., Jung, M., Liu, J., Osterman, G., O'Dell, C., Sparks, A., Butz, A., Guerlet, S., Yoshida, Y., Chen, H., and Gerbig, C.: Interpreting seasonal changes in the carbon balance of southern Amazonia using measurements of XCO₂ and chlorophyll fluorescence from GOSAT, *Geophysical Research Letters*, 40, 2829–2833, <https://doi.org/10.1002/grl.50452>, 2013.
- 25 Pillai, D., Buchwitz, M., Gerbig, C., Koch, T., Reuter, M., Bovensmann, H., Marshall, J., and Burrows, J. P.: Tracking city CO₂ emissions from space using a high-resolution inverse modeling approach: A case study for Berlin, Germany, *Atmospheric Chemistry and Physics*, 16, 9591–9610, <https://doi.org/10.5194/acp-16-9591-2016>, 2016.
- Reuter, M., Buchwitz, M., Schneising, O., Heymann, J., Bovensmann, H., and Burrows, J. P.: A method for improved SCIAMACHY CO₂ retrieval in the presence of optically thin clouds, *Atmospheric Measurement Techniques*, 3, 209–232, <https://doi.org/10.5194/amt-3-209-2010>, 2010.
- 30 Reuter, M., Buchwitz, M., Schneising, O., Krautwurst, S., O'Dell, C. W., Richter, A., Bovensmann, H., and Burrows, J. P.: Towards monitoring localized CO₂ emissions from space: co-located regional CO₂ and NO₂ enhancements observed by the OCO-2 and SSP satellites, *Atmospheric Chemistry and Physics Discussions*, 2019, 1–19, <https://doi.org/10.5194/acp-2019-15>, 2019.
- 35 Schneising, O., Heymann, J., Buchwitz, M., Reuter, M., Bovensmann, H., and Burrows, J. P.: Anthropogenic carbon dioxide source areas observed from space: assessment of regional enhancements and trends, *Atmospheric Chemistry and Physics*, 13, 2445–2454, <https://doi.org/10.5194/acp-13-2445-2013>, 2013.

- Schwandner, F. M., Gunson, M. R., Miller, C. E., Carn, S. A., Eldering, A., Krings, T., Verhulst, K. R., Schimel, D. S., Nguyen, H. M., Crisp, D., O'Dell, C. W., Osterman, G. B., Iraci, L. T., and Podolske, J. R.: Spaceborne detection of localized carbon dioxide sources, *Science*, 358, <https://doi.org/10.1126/science.aam5782>, 2017.
- 5 Sherlock, V., Connor, B., Robinson, J., Shiona, H., Smale, D., and Pollard, D. F.: TCCON data from Lauder (NZ), 120HR, Release GGG2014.R0, <https://doi.org/10.14291/tcon.ggg2014.lauder01.r0/1149293>, 2014a.
- Sherlock, V., Connor, B., Robinson, J., Shiona, H., Smale, D., and Pollard, D. F.: TCCON data from Lauder (NZ), 125HR, Release GGG2014.R0, <https://doi.org/10.14291/tcon.ggg2014.lauder02.r0/1149298>, 2014b.
- Sierk, B., Bézy, J.-L., Löscher, A., and Meijer, Y.: The European CO₂ Monitoring Mission: Observing anthropogenic greenhouse gas emissions from space, in: *International Conference on Space Optics – ICSO 2018*, edited by Sodnik, Z., Karafolas, N., and Cugny, B., vol. 11180, pp. 237 – 250, International Society for Optics and Photonics, SPIE, <https://doi.org/10.1117/12.2535941>, 2019.
- 10 Sussmann, R. and Rettinger, M.: TCCON data from Garmisch (DE), Release GGG2014.R2, <https://doi.org/10.14291/tcon.ggg2014.garmisch01.r2>, 2018a.
- Sussmann, R. and Rettinger, M.: TCCON data from Zugspitze (DE), Release GGG2014.R1, <https://doi.org/10.14291/tcon.ggg2014.zugspitze01.r1>, 2018b.
- 15 Té, Y., Jeseck, P., and Janssen, C.: TCCON data from Paris (FR), Release GGG2014.R0, <https://doi.org/10.14291/tcon.ggg2014.paris01.r0/1149279>, 2014.
- Thompson, D. R., Thorpe, A. K., Frankenberg, C., Green, R. O., Duren, R., Guanter, L., Hollstein, A., Middleton, E., Ong, L., and Ungar, S.: Space-based remote imaging spectroscopy of the Aliso Canyon CH₄ superemitter, *Geophysical Research Letters*, 43, 6571–6578, <https://doi.org/10.1002/2016GL069079>, 2016.
- 20 Thorpe, A. K., Frankenberg, C., Aubrey, A. D., Roberts, D. A., Nottrott, A. A., Rahn, T. A., Sauer, J. A., Dubey, M. K., Costigan, K. R., Arata, C., Steffke, A. M., Hills, S., Haselwimmer, C., Charlesworth, D., Funk, C. C., Green, R. O., Lundeen, S. R., Boardman, J. W., Eastwood, M. L., Sarture, C. M., Nolte, S. H., Mccubbin, I. B., Thompson, D. R., and McFadden, J. P.: Mapping methane concentrations from a controlled release experiment using the next generation airborne visible/infrared imaging spectrometer (AVIRIS-NG), *Remote Sensing of Environment*, 179, 104–115, <https://doi.org/10.1016/j.rse.2016.03.032>, 2016a.
- 25 Thorpe, A. K., Frankenberg, C., Green, R. O., Thompson, D. R., Aubrey, A. D., Mouroulis, P., Eastwood, M. L., and Matheou, G.: The Airborne Methane Plume Spectrometer (AMPS): Quantitative imaging of methane plumes in real time, in: *IEEE Aerospace Conference Proceedings*, vol. 2016-June, <https://doi.org/10.1109/AERO.2016.7500756>, 2016b.
- Warneke, T., Messerschmidt, J., Notholt, J., Weinzierl, C., Deutscher, N. M., Petri, C., and Grupe, P.: TCCON data from Orléans (FR), Release GGG2014.R0, <https://doi.org/10.14291/tcon.ggg2014.orleans01.r0/1149276>, 2014.
- 30 Wennberg, P. O., Wunch, D., Roehl, C. M., Blavier, J.-F., Toon, G. C., and Allen, N. T.: TCCON data from Caltech (US), Release GGG2014.R1, <https://doi.org/10.14291/tcon.ggg2014.pasadena01.r1/1182415>, 2015.
- Wennberg, P. O., Roehl, C. M., Blavier, J.-F., Wunch, D., and Allen, N. T.: TCCON data from Jet Propulsion Laboratory (US), 2011, Release GGG2014.R1, <https://doi.org/10.14291/tcon.ggg2014.jpl02.r1/1330096>, 2016a.
- Wennberg, P. O., Wunch, D., Roehl, C. M., Blavier, J.-F., Toon, G. C., and Allen, N. T.: TCCON data from Lamont (US), Release GGG2014.R1, <https://doi.org/10.14291/tcon.ggg2014.lamont01.r1/1255070>, 2016b.
- 35 Wennberg, P. O., Roehl, C. M., Wunch, D., Toon, G. C., Blavier, J.-F., Washenfelder, R., Keppel-Aleks, G., Allen, N. T., and Ayers, J.: TCCON data from Park Falls (US), Release GGG2014.R1, <https://doi.org/10.14291/tcon.ggg2014.parkfalls01.r1>, 2017.

- Wu, L., Hasekamp, O., Hu, H., Landgraf, J., Butz, A., aan de Brugh, J., Aben, I., Pollard, D. F., Griffith, D. W. T., Feist, D. G., Koshelev, D., Hase, F., Toon, G. C., Ohyama, H., Morino, I., Notholt, J., Shiomi, K., Iraci, L., Schneider, M., de Mazière, M., Sussmann, R., Kivi, R., Warneke, T., Goo, T.-Y., and Té, Y.: Carbon dioxide retrieval from OCO-2 satellite observations using the RemoTeC algorithm and validation with TCCON measurements, *Atmospheric Measurement Techniques*, 11, 3111–3130, <https://doi.org/10.5194/amt-11-3111-2018>, 2018.
- 5
- Wu, L., Hasekamp, O., Hu, H., aan de Brugh, J., Landgraf, J., Butz, A., and Aben, I.: Full-physics carbon dioxide retrievals from the OCO-2 satellite by only using the 2.06 μm band, *Atmospheric Measurement Techniques Discussions*, 2019, 1–15, <https://doi.org/10.5194/amt-2019-218>, <https://www.atmos-meas-tech-discuss.net/amt-2019-218/>, 2019b.
- Wu, L., aan de Brugh, J., Meijer, Y., Sierk, B., Hasekamp, O., Butz, A., and Landgraf, J.: XCO₂ observations using satellite measurements with moderate spectral resolution: Investigation using GOSAT and OCO-2 measurements, *Atmospheric Measurement Techniques Discussions*, 2019, 1–23, <https://doi.org/10.5194/amt-2019-232>, <https://www.atmos-meas-tech-discuss.net/amt-2019-232/>, 2019a.
- 10
- Wunch, D., Toon, G. C., Blavier, J.-F. L., Washenfelder, R. A., Notholt, J., Connor, B. J., Griffith, D. W. T., Sherlock, V., and Wennberg, P. O.: The Total Carbon Column Observing Network, *Philosophical Transactions of the Royal Society of London A: Mathematical, Physical and Engineering Sciences*, 369, 2087–2112, <https://doi.org/10.1098/rsta.2010.0240>, 2011a.
- 15
- Wunch, D., Wennberg, P. O., Toon, G. C., Connor, B. J., Fisher, B., Osterman, G. B., Frankenberg, C., Mandrake, L., O’Dell, C., Ahonen, P., Biraud, S. C., Castano, R., Cressie, N., Crisp, D., Deutscher, N. M., Eldering, A., Fisher, M. L., Griffith, D. W. T., Gunson, M., Heikkinen, P., Keppel-Aleks, G., Kyrö, E., Lindenmaier, R., Macatangay, R., Mendonca, J., Messerschmidt, J., Miller, C. E., Morino, I., Notholt, J., Oyafuso, F. A., Rettinger, M., Robinson, J., Roehl, C. M., Salawitch, R. J., Sherlock, V., Strong, K., Sussmann, R., Tanaka, T., Thompson, D. R., Uchino, O., Warneke, T., and Wofsy, S. C.: A method for evaluating bias in global measurements of CO₂ total columns from space, *Atmospheric Chemistry and Physics*, 11, 12 317–12 337, <https://doi.org/10.5194/acp-11-12317-2011>, 2011b.
- 20
- Yang, D., Liu, Y., Cai, Z., Chen, X., Yao, L., and Lu, D.: First Global Carbon Dioxide Maps Produced from TanSat Measurements, *Advances in Atmospheric Sciences*, 35, 621–623, <https://doi.org/10.1007/s00376-018-7312-6>, 2018.